Antisense inhibition of *accA* suppressed *luxS* expression that is essential for quorum sense signaling, biofilm formation, and virulence

Tatiana Hillman[1]
[1]Biotechnology, TheLAB, Inc., Los Angeles, California, United States
Corresponding author: Tatianna Hillman[1]
E-mail: thillman@usc.edu

ABSTRACT

Bacterial multiple drug resistance is a significant issue for the medical community. Gram-negative bacteria exhibit higher rates of multi-drug resistance. Gram-negative bacteria are more resistant to multiple antibiotics partly because of the impermeability of the gram-negative bacterial cell wall and cell envelope that consists of a double membrane. The double membrane limits an increased and internal accumulation of antibiotics. The double-membrane has an outer membrane and an inner membrane. The outer membrane of lipopolysaccharides regulates the transport of hydrophobic molecules as the inner membrane controls the influx of hydrophilic particles. The inner plasma membrane consists of phospholipids configured during fatty acid synthesis. The transcription of *accA* produces the acetyl-CoA carboxylase transferase enzyme required for catalyzing the output of fatty acids and phospholipids. To increase antibiotic susceptibility and decrease the growth of Escherichia coli, fatty acid synthesis was interrupted to disrupt the composition of the inner membrane. The gene *accA* was inhibited with antisense RNA and produced a qPCR product of 63 ng/µL. The inhibition of *accA* suppressed the expression of *luxS*. The *luxS* gene is a vital virulence factor for regulating cell growth, transferring intercellular quorum-sensing signals called autoinducer-2, and for forming biofilm. Bacterial cells that expressed antisense inhibition of *accA* displayed a higher magnitude of antibiotic susceptibility. The results confirm *accA* as a potent target for developing novel antibiotics such as antimicrobial gene therapies.

Keywords: Antibiotic Resistance, Antibiotics, Biofilm, Carboxylase Enzymes, Autoinducers, Quorum Sensing, Antisense RNA, and Fatty Acid Synthesis

INTRODUCTION

Multiple drug resistant (MDR) bacteria present an enormous challenge for many medical communities and organizations, globally. For Example, *A. baumanii* is an MDR-gram negative bacterium *that* inhabits hospitals. *A. baumanii* bacteria cause 64% of urinary tract infections during the use of catheters [7]. Multiple drug resistance occurs when one bacterium is resistant to more than one antibiotic. Gram-negative bacteria produce a majority of multiple drug resistant bacterial infections. The cell envelope of gram-negative bacteria plays a prominent role in antibiotic resistance. The cell envelope of gram-negative bacteria consists of a phospholipid inner membrane, a periplasmic space, and an outer membrane. The cell envelope contains an inner membrane containing a phospholipid bilayer and an outer membrane with a lipopolysaccharide region termed the LPS. Due to this double membrane, gram-negative bacteria are partially protected from diffusible hydrophobic and hydrophilic compounds. LPS blocks the influx of hydrophobic molecules, and the IM phospholipid bilayer limits the internal transport of hydrophilic molecules. The structure of the double membrane for gram-negative bacteria causes antibiotic drug discovery to become an arduous task [8]. The double-layer limits the accrual of antibiotics and enzyme inhibitors into the gram-negative bacterial cell.

The inner membrane (IM) for gram-negative bacteria is composed of a phospholipid bilayer, and the phospholipid (PL) bilayer is produced by the fatty acid type II synthesis pathway [8]. The first phase of FASII includes the carboxylation of acetyl-CoA, which forms into malonyl-CoA through a biotin carboxylase carrier protein (BCCP) and the acetyl-CoA carboxylase transferase (CT) enzyme. To begin the process of FASII, a change from malonyl-CoA into malonyl-ACP is required. Malonyl-ACP combines with acetyl-CoA to generate acetoacetyl-ACP by the FabH enzyme. After FASII is initiated, two carbons are added per every cycle of fatty acid elongation that includes the conversion of malonyl-ACP into acyl-ACP. Acetyl CoA combines with a carboxyl group to form malonyl-CoA in an ATP-dependent reaction [9]. Bacterial fatty acids synthesis produces phospholipids required to stabilize and form plasma membranes.

CT catalyzes the elongation of fatty acids. The gene *accA* encodes the AccA domain of the CT subunit. The acetyl-CoA carboxylase complex is an essential enzyme for the first-rate limiting step in fatty acid synthesis. The ACCase enzyme has three subunits that include a biotin carboxylase (BC), biotin carboxyl carrier protein (BCCP), and an α2β2heterotetrameric carboxyltransferase (CT) [16]. The *accB* codes for BCCP and BC is translated from *accC*. The *accB* and *accC* (*accBC*) are transcribed simultaneously by the *accBC* mini operon [17]. The genes *accA* and *accD* encode the α-subunits and β-subunits, respectively. The α-subunit (*accA*) and β-subunit (*accD*) make up the CT portion of ACCase. Bacterial cells use enzymes that lyse glucose molecules into pyruvates. The ACCase complex subunit, termed AccA, transfers a carboxyl delivered through BC-BCCP to CT. The BC-BCCP positions a

carboxyl from a pyruvate to the CT. The CT orients the carboxyl to acetyl-CoA that forms a malonyl-CoA.

Bacterial fatty acid synthesis can significantly impact the production of biofilm and antibiotic susceptibility. More research is needed to further elucidate the link between the phospholipid membrane and the condition of a biofilm [28]. However, Yao and Rock confirmed the significant connection between biofilm formation and fatty acid synthesis enzymes contained in the structure of *S. aureus* [39]. A biofilm includes tight junctional communities of bacterial cells that have an extracellular matrix type of outer covering [13]. The cover of the extracellular matrix allows bacteria to attach to a biotic or abiotic surface. This extracellular matrix protects bacterial cells from external and environmental pressures. However, the metabolic fluxes that affect bacterial biofilm formation are not fully elucidated and understood [13]. The link between bacterial metabolism and virulence needs further elucidation. For this reason, *accA* genes were silenced, which disrupts fatty acid synthesis, to demonstrate the link between bacterial FA metabolism and the creation of biofilm, a major virulence factor.

accA was suppressed with interfering antisense RNAs (asRNAs) (Fig 1), and then its gene expression was quantified via Real-Time PCR (qPCR). The asRNAs were bound to sequences flanking the ribosome-binding site and the start codon for the 150-base pair (bp) *accA* target mRNAs. The antisense RNA blocks ribosomal detection through the ribosomal binding site (RBS) and inhibits translation [10]. D-Glucose was also added to positive asRNA *accA* ((+)asRNA-accA) expressing *E.coli* cultures to affirm the interaction between the catabolism of glucose into carboxyls and *accA* gene expression. The (+)asRNA-*accA* inhibited *E.coli* cells enhanced with glucose molecules were then prepared for RNA isolation to perform qPCR of accA (qPCR-accA). accA encodes the AccA subunit of the acetyl-CoA carboxylase transferase enzyme (CT), so by using antisense RNA transcripts to inhibit *accA,* the CT enzyme lacked the AccA subunit needed for FA catalysis and production. Inhibiting *accA* with asRNA transcripts interrupts the activation of FA synthesis where less production of FAs may negatively distort the composition of the IM phospholipid bilayer, which can increase the influx of hydrophilic antibiotics across the IM and reduce biofilm consistency.

LuxS, an autoinducer-2 (AI-2) producing S-ribosyl homocysteine lyase protein, is also required for biofilm formation and a study demonstrated that the growth of biofilm temporally was suppressed in the absence of viable nutrients (i.e. glucose) within the interior of *B. subtilis* cells [13]. Zuberi et al. applied CRISPRi technology to inhibit *luxS* genes in *E. coli* cells and found that biofilm formation depended upon the expression of *luxS*. They used a crystal violet test to assess the effect of *luxS* on biofilm. Biofilm formation decreased as *luxS* expression was reduced [53]. LuxS produces AI-2 using 4,5,-dihydroxy-2,3-pentadione (DPD) as a precursor. AI-2 is a released signaling molecule that induces quorum sense (QS) through bacterial cell-to-cell interactions. The AI-2 signaling molecule monitors metabolism, assists with forming a biofilm,

allows the transport of metabolite molecules, and transports regulatory signals [32]. Lux-S and (+)asRNA-accA inhibitors of FASII can each affect bacterial biofilm formation.

This study attempts to ascertain possible interdependent activity between *accA* and *luxS*. To analyze a potential synergy between *accA* and *luxS*, E. coli (+)asRNA-accA transformants were exposed to glucose molecules, *and* then the qPCR products of *luxS were* quantified (luxS-qPCR). In addition, to test for the antibiotic susceptibility of *E. coli*, tetracycline, carbenicillin, and chloramphenicol-containing disks were implanted in *E. coli*(+)asRNA-*accA* expressing cell cultures. Two main hypotheses were tested in this study including: 1) silencing *accA* and lessening glucose availability decreases *luxS* expression that is an essential component of the LuxS/AI-2 QS system necessary for biofilm creation, and 2) inhibiting *accA* heightens antibiotic susceptibility of gram-negative bacteria because its suppression degrades the IM via FASII disruption. Therefore, the purpose of this study includes displaying a connection between bacterial metabolism (glucose-accA-FASII) and virulence (i.e. accA-luxS activity). The aim is to also demonstrate *accA* as an advantageous target for designing novel antimicrobial gene therapies to ablate its expression.

Figure 1 Plasmid Assembly and Gene Silencing of *accA*

Plasmid Assembly and Gene Silencing of the PCR products and the PTasRNA expression vector of the plasmid pHN1257 were digested with the restriction enzymes XhoI (upstream) and NcoI (downstream). After the restriction digestion, the antisense PCR product was ligated into the IPTG-PTasRNA inducible vector of pHN1257 at the multiple cloning site.

doi: 10.3390/ijms15022773, this article is an open-access article distributed under the terms and
conditions of the Creative Commons Attribution license (http://creativecommons.org/licenses/by/3.0/).
https://www.ncbi.nlm.nih.gov/pmc/articles/PMC3958881/figure/f6-ijms-15-02773/

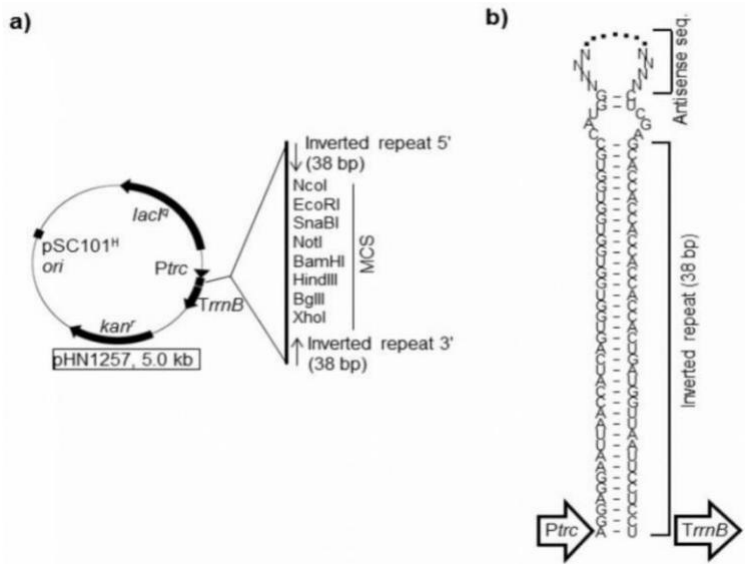

MATERIALS AND METHODS
BACTERIAL CELL CULTURE AND RNA EXTRACTION

The *Escherichia coli* TOP10 strain of cells was cultured and plated on 25 mL agar plates. The bacterial cells were inoculated into Luria-Bertani broth, enhanced with glucose concentrations of 200µM, 50µM, and 0µM. The cultures of 200, 50, and 0 micromolar (n=7) of glucose were measured for dsDNA and RNA OD260 concentrations and replicated seven times. Varying levels of glucose, including 15mM, 7.5mM, 5mM, and a control of glucose, were added to LB liquid with *Escherichia coli* cells. The plasmid pHN1257 was utilized to assemble the antisense expression vectors.

The recombinant plasmid pHN1257 for the expression of antisense RNA was plated with the kanamycin antibiotic and incubated at 37°C for 24 h. Cells grown on agar plates were inoculated into 4 mL of LB liquid media with (+) and (-) PTasRNA bacterial cells expressing asRNA for *accA* cultured with kanamycin. A total of 20 RNA extractions were completed with the Omega E.Z.N.A bacterial extraction kit.

cDNA PREPARATION

The author used the OneScript Reverse Transcriptase cDNA Synthesis kit by Applied Biological Materials Inc. or ABM. Approximately, 1µg of RNA from each sample, high glucose, medium glucose, low glucose, and (-) glucose were added to 0.5µM oligonucleotides(dT) (10µM). For asRNA and (-) RNA, 1 **µg** of each total RNA extract was added to the initial primer/RNA and reaction mixture. cDNA was also prepared for *luxS* quantification. The original primer/RNA mix consisted of 1µg of total RNA, 1µL of oligo(dt), 1µL of dNTP (10mM) mix, and nuclease-free water for a 20µL reaction solution.

PCR

A Promega PCR MasterMix kit at a volume of 25µL was added to the upstream and downstream primers, each of 0.5µL specific for the *accA* gene target. PCR amplification was repeated in triplicate. The concentrations of the two cDNA samples added to the PCR master mix were 190ng and 230ng plus nuclease-free water. A 2X and 1X upstream primer, 10µM 0.5– 5.0µl0.1–1.0µM, and a downstream primer, 10µM 0.5 to 5.0µl 0.1 to 1.0µM, DNA template 1–5µl less than 250ng, and nuclease-free water were mixed into a 50µl PCR reaction mixture. The PCR thermocycler completed 40 cycles of amplification instead of 35 cycles.

AGAROSE GEL ELECTROPHORESIS AND PLASMID ASSEMBLY

The conditions of the PCR products, without primer dimers and contamination for the target gene *accA,* were detected through agarose gel electrophoresis. The PCR products were confirmed without primer dimers, and contamination, the PCR products, and the PTasRNA expression vector of the plasmid pHN1257 were digested with the restriction enzymes XhoI (upstream) and NcoI (downstream) (New England Biolabs XhoI- catalog R0146S- 1,000 units and NcoI- catalog R0193S- 1,000 units) (Fig. 1).
Each microcentrifuge tube was placed in an incubator for 30 min at 37°C. A heat block was heated to 90°C. The PCR products of the *accA* gene were ligated into the pHN1257 plasmid by mixing 1µL of the DNA insert with 2µL of the plasmids, adding 5µL of the ligation mix, and then placing the tubes into a heat block at 90°C for 15 min (Takara Ligation Kit 6023).

REAL-TIME PCR

The author enhanced each bacterial sample with glucose concentrations of 15mM, 7.5mM, 5mM, and 0mM (n=3). The cDNA from H-glucose, M-Glucose, L-glucose, and the control (-) glucose was diluted in a 1:8 serial dilution. A 10-fold dilution of standards was prepared for bacterial samples transformed with (+) asRNA-inducible plasmids and exposed to high to low volume of glucose. The amount of gene expression for *accA* and the target gene *luxS* was measured using absolute quantification methods of qPCR. The diluted cDNA was pipetted into a transparent 96 well plate. A 0.4µL of each primer pair mixture was pipetted into a microcentrifuge tube with 10µL of SensiMix SYBR MasterMix, and with 1.2µL of DEPC water. The SYBR reaction mixture of 12µL was then pipetted into the wells with diluted and undiluted cDNA. The optical film was sealed to the plate. The PCR plates were centrifuged for 2 min at 2500 rpm to reposition all liquids to the bottom of the wells. The real-time PCR amplification protocol from the Roche Lightcycler 480 was used.

THE qPCR ABSOLUTE QUANTIFICATION OF LUX-S

Bacterial cells were transformed with the pHN1257 plasmid expressing asRNA to inhibit the genetic expression of *accA*. Triplicates of qPCR were performed to quantify the gene copies of *luxS*. The author added 25µM and 5µM concentrations of glucose to the bacterial samples expressing antisense RNA for the inhibition of the gene *accA.* RNA was extracted from cells grown with 25µM glucose and 5µM glucose. The cells grown with glucose in the medium were also transformed with antisense expressing IPTG-PT-asRNA inducible pHN1257plasmids. Cells were cultured without (-) glucose, but the expression of *accA* was also inhibited (+) asRNA. A control without (-) glucose and (-) asRNA was compared for each sample. The number of gene copies for *luxS* was measured using the qPCR amplification protocol and absolute quantification (Roche Lightcycler 480).

ANTIBIOTIC RESISTANCE TEST

Competent T7 bacteria cells were transformed with the inducible vector termed pHN1257, expressing antisense RNA to inhibit the gene *accA.* The newly remodeled bacterial cells were plated in nutrient agar medium consisting of the antibiotic kanamycin. Three to five colonies from the pHN-1257-asRNA-*accA* bacterial transformants were selected and cultured in LB broth, enhanced with kanamycin for 18 to 24 h at 37°**C** in a shaking incubator. A control group that did not express asRNA for *accA* was cultured in LB broth overnight at 37°**C**. One hundred microliters of the pHN1257- asRNA-*accA* and from the control group

were pipetted into nutrient agar Petri dishes (N=64) containing 50 micromolar of kanamycin (50µg/mL) antibiotic for the sample of pHN1257-asRNA-*accA*. A swab was used to spread 100**µL** of each experimental (with asRNA) and the control (without asRNA) onto the agar plates to form a lawn of bacterial growth. The six-millimeter-sized disks contained five microliters for each of the three consecutive antibiotics, including tetracycline (10µg/mL), carbenicillin (100µg/mL), and chloramphenicol (25µg/mL). Each group of eight disks was prepared with tetracycline carbenicillin, and chloramphenicol. The antibiotic disks were placed on the agar plates. The bacterial cultures grew for 18-24 h at 37oC. The zone of inhibition for each of the disc (N=64) were measured in mm and compared to specific criteria for determining antibiotic resistance and susceptibility of bacteria.

STATISTICAL ANALYSIS

The figures were constructed with the Sigma Plot 14th edition, Microsoft excel, and the 8th edition of GraphPad Prism. The mean and standard deviations were calculated by Microsoft Excel and GraphPad Prism. The p-values and the ANOVA results were produced through GraphPad Prism. The standard curves for the absolute quantification of the genes accA and luxS were generated through Microsoft excel with linear regression coefficients added and calculated for each standard curve for the absolute quantification of accA and luxS. The antibiotic resistance test was analyzed, given descriptive statistics, and generated paired-t-test results through the OriginPro 2019B software. A t-test and a density graph for antibiotic susceptibility of pHN1257(+) asRNA for accA was produced through OriginPro 2019B.

RESULTS AND DISCUSSION

THE EFFECT OF GLUCOSE ON THE RNA CONCENTRATION AND THE EXPRESSION OF *accA*

To observe the effect of extracellular glucose on intracellular RNA transcription and *accA* expression, glucose was added to *Escherichia coli* liquid cultures. As the glucose concentration increased, the transcription of *accA* was amplified. After culturing *Escherichia coli* with varied concentrations of glucose, the RNA concentrations for each sample measured were 1392, 797, 608, and 199 ng/µL for H-Glucose (15mM) , M- Glucose (7.5mM), L-Glucose (5mM), and the control, respectively, (Fig 3). The RNA of each bacterial sample enhanced with glucose was extracted, and the concentrations determined (N=20, 335.4 ± 329.2). The level of *accA* by qPCR analysis, in units ng/µL, included: 4210, 375, 1500, and 196 for H-glucose, M-glucose, L-glucose, and for the control, respectively, (Fig 3).

After loading a 96-well plate with 8-fold dilution standards for each sample, the standards of each sample were used to calculate a standard curve. The standard curves were used to perform absolute qPCR quantification of *accA* gene copies. The number of qPCR *accA* products ranged from 11-186, 5-18, and 0-79 gene copies for high-glucose, medium-glucose, and low-glucose/control, respectively, (N=12, 48±38). When comparing 200 µM-glucose bacterial samples to the control groups, the difference between the samples was statistically significant (p=0.038) (Figs 3-4). The cells grown at 200µM of glucose yielded a more substantial and excessive yield of dsDNA than cells cultured without glucose (Figs 3-4).

The augmentation of RNA transcription through glucose supplementation occurred because increased carbon uptake induces intensified *accBC* and *accD*1 transcription, and by controlling the flux of the tricarboxylic acid (TCA) cycle augments the production of malonyl-CoA [20]. More available carbon nutrients from glucose addition increased the transcription of *accA,* as reflected in the qPCR results (Fig 5). Adding glucose to the liquid cultures increased the production of

accA qPCR products. If *accA* expression was amplified, then the activity of the CT transferring carboxyl to acetyl-CoA for conversion into malonyl-CoA also surged. Acetyl-CoA carboxylase (ACC) is a biotin-dependent carboxylase. The ACCase complex consists of a biotin carboxylase (BC), carboxyltransferase (CT), and a biotin-carboxyl carrier protein (BCCP) subunit. The BC of *E. coli* is bonded into a dimer (Fig 2).

Figure 2 BC of *E. coli* is bonded together in a dimer (*Retrieved from Reference 19)***.*** Each dimer has an active site oriented at 25Å from the region of interaction. This dimer interface is composed of distant communications between each of the two active sites in a dimer. The two monomers of the BC dimer may share the responsibility of inducing catalysis. One of the BC monomers can bind the substrate during its initiation of the reaction, while the second monomer disperses the product.

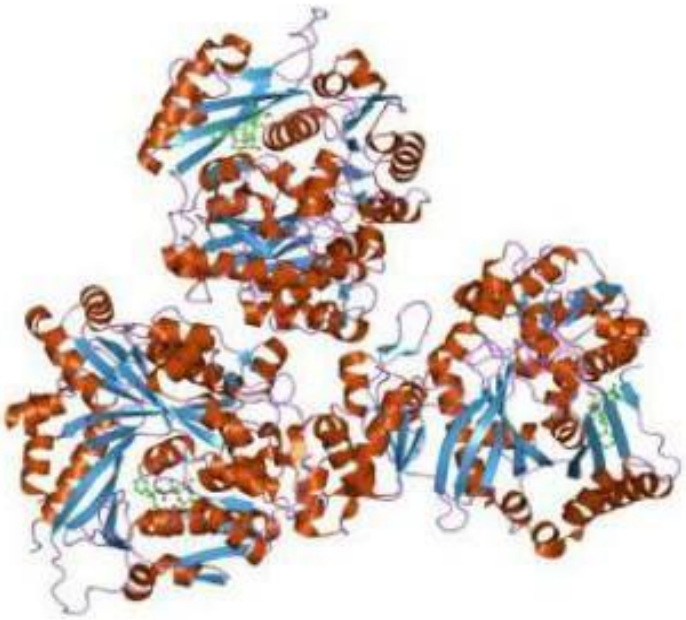

Figure 3 Glucose concentration versus RNA Glucose concentrations of 15mM, 7.5mM, and 5mM with the control samples each yielded RNA concentrations in ng/µL, 1392, 797, 608, and 179, respectively. A) The bacterial sample with 15mM glucose yielded the highest substantial measure of RNA, noting a proportional relationship between glucose and genetic expression of *E. coli*. B) The results display the qPCR results for 15mM, 7.5mM, 5mM, and control. The samples with 15mM and 5mM glucose showed the highest genetic activity of *accA* transcription, measuring *accA* concentrations of 4,210 ng/µL and 1,500 ng/µL, respectively. The *accA* qPCR concentrations for 7.5mM *accA* equaled 372 ng/µL and 196 ng/µL quantities for the control. C) The analysis displays the OD260 measure of DNA results for samples of *E. coli* grown in medium enhanced with 200µM, 50µM, and 0µM of glucose.

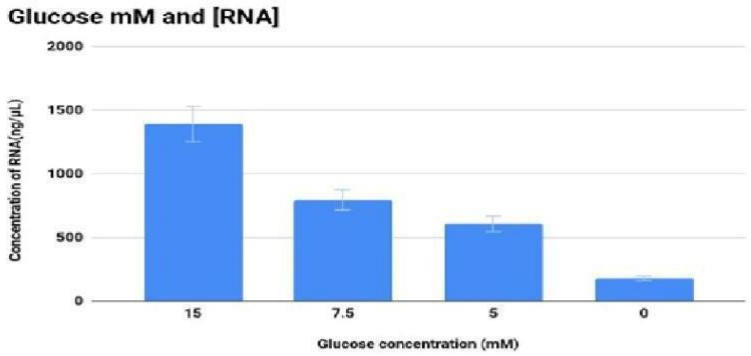

A)

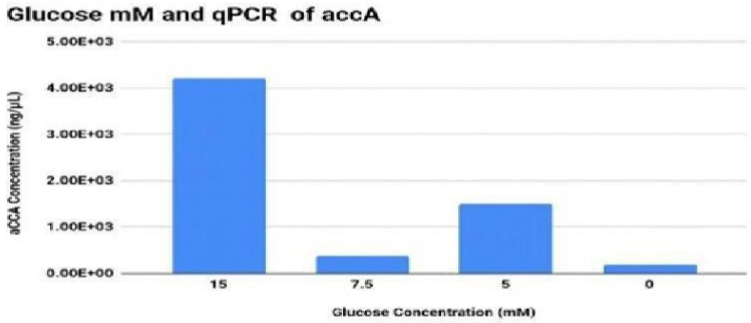

B)

C)

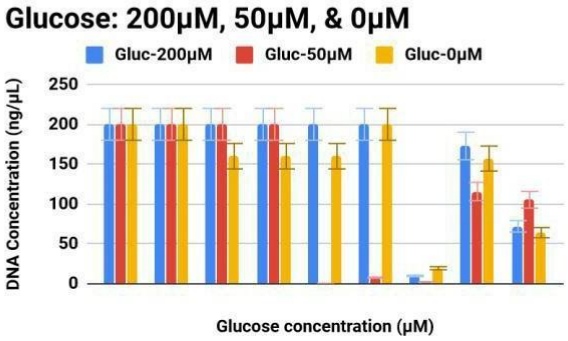

Figure 4, RNA Concentrations vs. Glucose Concentration A) The enhanced *E. coli* bacteria cultures (n=3) with 200µM, 50µM, and a control of glucose (59±49). B) 50µM of glucose in a bacterial sample, the highest yield was 566ng/µL, for 200µM, 117ng/µL of RNA was produced, and the control measured to 76ng/µL of RNA.

A)

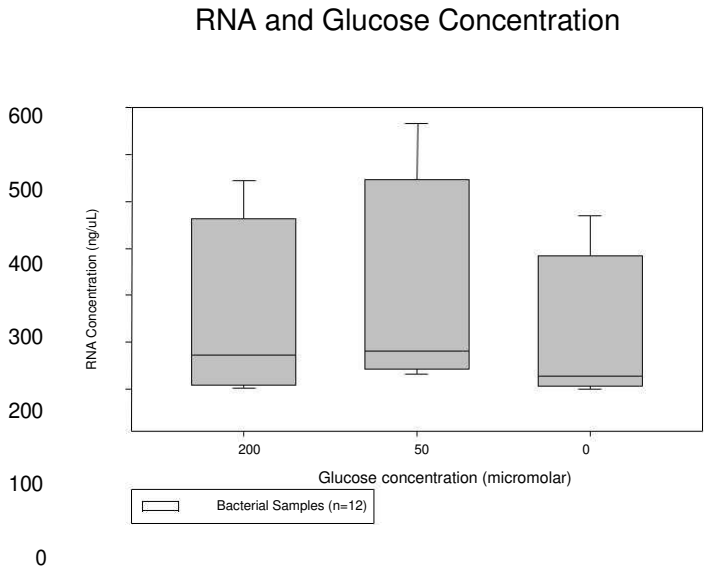

B)

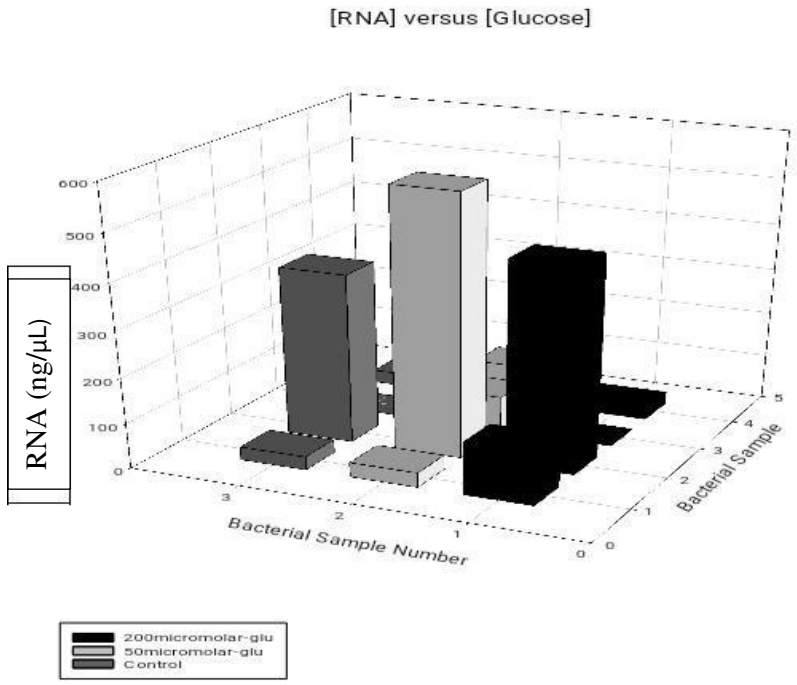

Figure 5 Predicted and Actual Residuals A) The QQ plot of RNA concentration versus *accA* exhibits means that are normally distributed. B) The homoscedasticity of [RNA] and [*accA*] is non-linear due to the size of error that varies across values of [RNA] and *[accA*]. C) The residual plot resembles heteroscedasticity where residuals increase as the predicted values move from 0 to 800 ng/µL for [RNA] and [*accA*].

A) B) C)

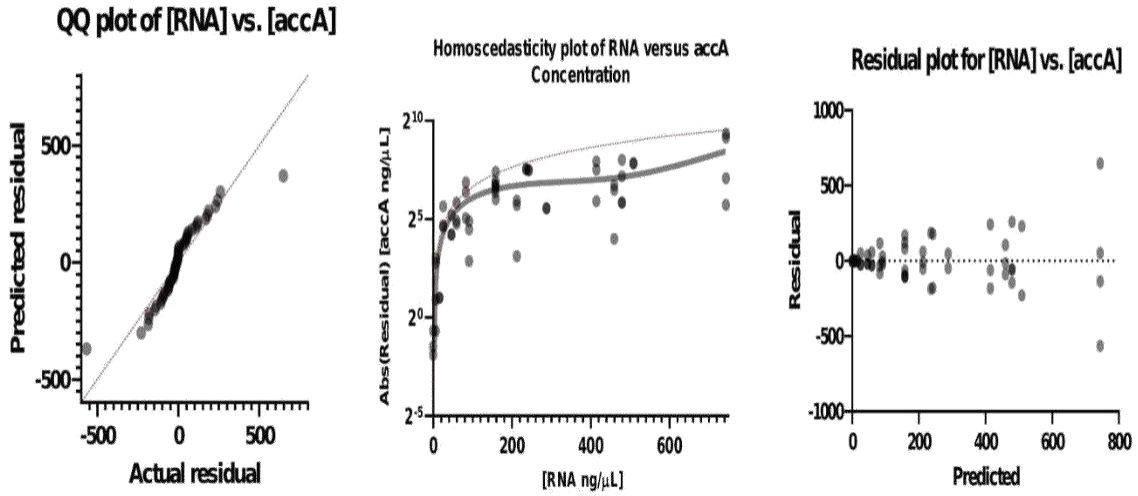

The biotin-dependent ACCase enzyme performs a crucial function for catalyzing fatty acid metabolic activity. The ACC complex completes two enzymatic reactions in two half-reaction steps. The first step is catalyzed by a biotin carboxylase (BC) that carboxylates an N1' atom of a biotin vitamin cofactor, utilizing ATP and carbon dioxide from bicarbonate [18]. Biotin or vitamin H covalently bonds to a lysine side chain residue located in the biotin carboxyl carrier protein of the BCCP subunit. The second step uses a carboxyl transferase (CT) to transfer carbon dioxide from a carboxybiotin to a carboxyl group. The increased glucose supplementation provided excess carboxyl groups and ATP needed for the BCCP of an *E. coli* ACC to use its thumb appendage (Fig 6). As biotin binds to the BCCP, the thumb attaches to biotin. The thumb fortifies the BCCP, tightening the bond between biotin and the BCCP. By increasing the glucose supplementation, more energy from ATP was available for the ACCase enzyme to link the BCCP thumb to biotin.

Eliminating one of the dimers of BC renders it inactive. Each dimer has an active site oriented at 25Å from the region of interaction of the dimer [18]. This dimer interface is composed of distant communications between each of the two active sites. The two monomers of the BC dimer may share the responsibility of inducing catalysis. One of the BC monomers can bind the substrate during the initiation of the reaction, while the second monomer disperses the product. However, the BC dimer during the first half-reaction does not exhibit cooperative behavior confirmed by enzyme kinetics analysis.

Biotin carboxylase has 449 amino acid side chain residues. The 449 residues of BC are split into three domains. The three domains include a domain at the N- terminus, an ATP-grasp or a B-domain, and a C-terminal domain. The Met1-lle103 residues represent the N-terminal domain that consists of a β-sheet, five parallel strands, and four α-helices. The ATP-grasp contains the residues Val131-Tyr203, 3 β-sheets, and two α-helices [16]. BC has residues Arg208-Lys449 in its C-terminal domain. The BC subunit is composed of 8 antiparallel β-sheets, 3 antiparallel β-sheets, and 7 α-helices [16]. Each monomeric section of the BC dimer has an active site where the residues are not shared between monomers.

Glucose also provided the carboxyl groups required for the BCCP to transfer a carboxyl to CT. The BCCP of bacteria closely resembles the ACC2 of human ACC, but human ACC2 does not contain a thumb extension [18]. Human BCCP is less restricted and can interact more with the BCCP of *E. coli*. In humans, the presence of a thumb inhibits biotin from binding to the human holocarboxylase synthetase or HCS [18]. However, in *E. coli,* the thumb does not interfere with biotin, forming a bond with an enzyme called *E. coli* BirA. Biotin is needed for all biotin-dependent carboxylase reactions.

Figure 6, The BCCP of *E. coli* ACC uses a thumb appendage (*retrieved from reference 23***).A)** The "thumb" of a BCCP. **B)** As biotin binds to the BCCP, the thumb attaches to biotin. **C)** The BCCP transfers the carboxyl to the CT. The thumb fortifies the BCCP, tightening the bond between biotin and the BCCP.

(BCCP)

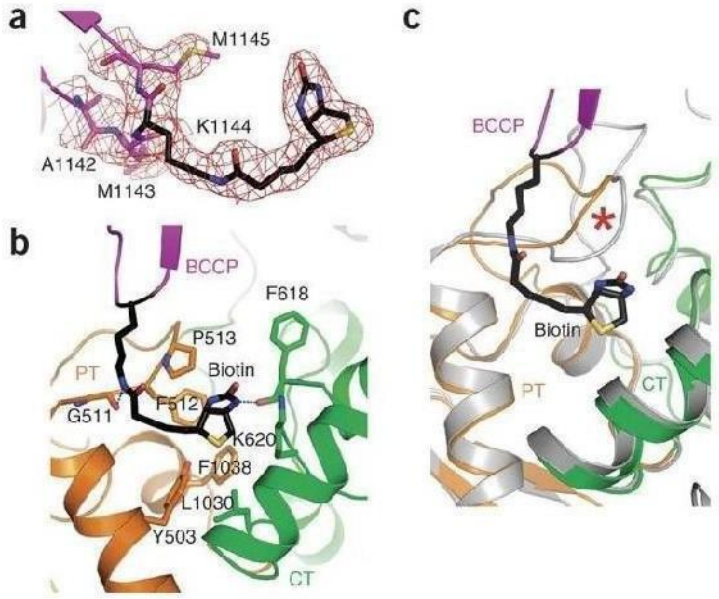

If a carboxyl is not present, then biotin cannot attach to the CT subunit [21]. This prevents the loss of ATP as a source of energy for BC-to-CT coupling reactions. The *E. coli* samples that were enhanced with glucose produced the highest concentration of *accA* and RNA because the glucose produced more ATP for the BC-to-CT interaction to occur. The glucose contained increased pyruvate molecules that yielded more carboxyl groups and ATP for the BC-CT interaction. The increased access of carboxyl groups induced the amplified attachment of biotin to the CT. The CT subunit has an N and a C domain. Each of the two subunits has a crotonase fold, which is a β-β-α superhelix [18]. At the interface of the CT dimer, there is an active site present.

The CT subunits are α2β2 heterotetramers [18]. The CT subunits are required to bond as a dimer to activate CT and catalyze the second half-reaction (Fig 7). The X-ray crystal structure of the CT shows a bond between the intermediate and the product of the response [21]. Every biotin-dependent enzyme requires two half-reactions that have structurally isolated and separated active sites [21]. It has been confirmed that separated active sites are physically produced in this orientation to regulate the interaction with biotin, which stabilizes the interaction of biotin with the BC to CT reactions. BC, BCCP, and CT mimic a ping-pong-ball-type interaction over a distant gap of separation between the carboxylase and transferase reactions [22].

Figure 7 The CT domain, has an N and a C domain (*this figure was retrieved from the Protein Data Bank of Europe and originally published in reference 23***).** Each of the two subunits has a crotonase-fold. This is a β-β-α superhelix (Tong, 2013.) At the interface of the CT dimer of its domain, there is an active site present. The CT subunits are α2β2 heterotetramers. The CT domains are required to bond as a dimer for the CT to be active and catalyze the second half-reaction. (color-grey=β/AccD, color-blue=α/AccA.)

(CT)

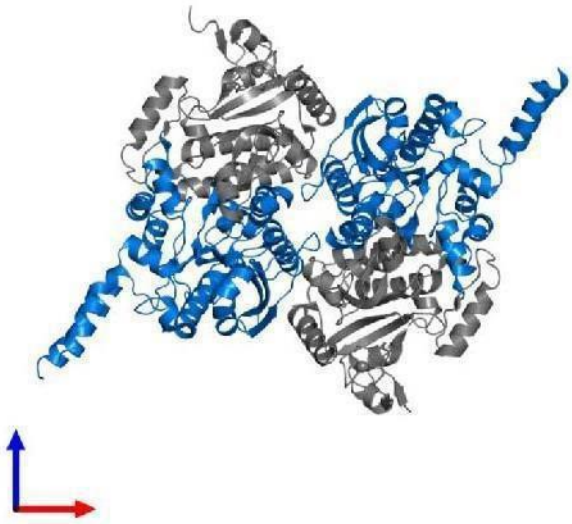

Normally, BC, BCCP, or CT are all bonded together as a multi-subunit protein or as separate domains. However, the orientation of the ACCase subunits rely on the type of organism and the class of the ACCase enzyme. BC and BCCP are conserved conformational structures. The conformation of the CT subunit, instead, depends on the behavior of the chemical substrates. The ACCase enzyme is biotin-dependent for catalyzing fatty acid synthesis. Biotin consists of a C, N, and a S cyclic ring linked to a five-carbon fatty acid chain. Biotin is a cofactor that is required for metabolism. Biotin is called vitamin H, which is bound to a lysine side chain residue of a biotin-dependent enzyme [24]. The biotin to protein bond assists with

carboxylation and decarboxylation activities. To catalyze the biotin-dependent carboxylase reactions, BC and CT must interact with the biotin cofactor. Bacterial ACCase enzymes encase four subunits: BC at 50kD, BCCP subunit with 17kD, and two subunits called alpha and beta, weighing at 33 kD for each component required for the CT reactions [18]. The ACCase enzyme has a stoichiometric ratio of 2:4:2 for BC, BCCP, and CTα with CTβ, respectively.

There was a reduction in *accA* and RNA activity because of the reduced availability of carboxyl groups after decreasing glucose supplementation. When carboxyl groups are supplied by glucose, the ATP-grasp of BC can appear as a closed conformation. When there are less carboxyl substrates bound to the biotin carboxylase, the ATP-grasp domain appears as an open conformation that extends from the primary protein structure. When the glucose was decreased, fewer carboxyl substrates could bind, and the ATP-grasp domain remained in an opened configuration. Reducing the volume of glucose provided less ATP availability.

Less ATP lowers the activity of ATP with the ATP-grasp monomer. When ATP binds to the ATP-grasp domain, it rotates at a 45° angle to capture the ATP and grasp it into its active site [17]. When the BCCP domain of human ACC2 was placed over the C-terminal alpha atoms of the image of the *E. coli* structure, the crystal violet image discovered the human ACC2 did not have a “thumb.” The “thumb” is a loop with eight amino acids that extend from the BCCP-C-terminus domain [17]. The BCCP and BC of *E. coli* become bound together at an angle of resolution equal to 2.49 Å [16]. The BCCP and BC are new sites that can be targeted with antibiotics to reduce the activity of acetyl-CoA carboxylase. When ablating *accA* gene expression, the alpha-subunit (AccA) of the CT for the ACCase enzyme can become absent, and disrupt the BC-to-CT interaction required for catalyzing fatty acid synthesis. Fatty acid synthesis is catalyzed by the CT conversion of acetyl-CoA into malonyl-CoA.

qPCR RESULTS OF THE ANTISENSE RNA INHIBITION OF TARGET GENE *accA*

For confirming the inhibition of *accA*, cells were transformed with pHN1257 plasmids carrying the insert for asRNA transcription of *accA*. The production of antisense RNA required the ligation of the PCR product for the gene insert, *accA,* into the plasmid pHN1257 (Fig. 1). The re-engineered pHN1257 amplified the expression of antisense RNA for *accA*. The total RNA concentration for the control (-) asRNA equaled 739.44 ng/µL. The control (-) asRNA yielded a miRNA concentration of 334.98 ng/µL. The RNA concentration for transformed bacterial cells with the asRNA of the *accA* pHN1257plasmid was 279.28ng/µL. The miRNA concentration of the cells with asRNA measured to 240.90 ng/µL. The gene of *accA* was successfully suppressed by asRNA in vitro with 63 ng/µL of qPCR measured for bacterial cells (n=3) transformed with recombinant antisense pHN1257 plasmid DNA (37.8 ± 35.6). The Real-Time PCR (qPCR) results for the

bacterial cells without the antisense gene target and insert yielded 421.69 ng/µL for *accA.* There was a 147 % (95% CI, [63, 421.69]) difference between cells without asRNA expression versus cells transcribing asRNA for *accA* (p=0.027).

Fatty acid synthesis requires catalysis by acetyl-CoA carboxylase transferase, which transfers a carboxyl to acetyl-CoA to produce malonyl-CoA [25]. The long-chain fatty acids are produced after the ACCase transferase, encoded in *accA and accD*, transfers a carboxyl group to acetyl-CoA, forming malonyl-CoA (Fig 8). This catalyzation requires energy from ATP, access to bicarbonate, and the vitamin H cofactor of biotin. ATP from glucose is the most significant source of energy that is needed for most metabolic activities. The inner membranes (IM) for gram-negative bacteria are composed of phospholipid bilayers. The phospholipid (PL) bilayer is produced by the fatty acid type II synthesis pathway [8]. The first phase of FASII includes the carboxylation of acetyl-CoA, which forms into malonyl-CoA through a biotin carrier protein (BCCP) and the acetyl-CoA carboxylase transferase (CT) enzyme.

To begin the process of FASII, the change from malonyl-CoA to malonyl-ACP is required. Malonyl-ACP combines with acetyl-CoA to generate acetoacetyl-ACP by the FabH enzyme. After FASII is initiated, two carbons are added per every cycle of fatty acid elongation through the conversion of malonyl-ACP into acyl-ACP. Fatty acid synthesis II or FASII includes separate subunits that interact. FASI proteins are expressed as cohesive and connected domains on a multi-polypeptide chain. *E. coli* has an acetyl-CoA carboxylase, which is a part of the FASII category.

The ACCase enzyme complex catalyzes the first step of fatty acid synthesis. The acetyl-CoA carboxylase consists of three subunits called biotin carboxylase, the biotin carboxyl carrier protein, and carboxyl transferase. The carboxyl transferase catalyzes the transfer of a carboxyl group to acetyl-CoA, producing malonyl-CoA. The biotin carboxyl vehicle and carrier have two domains. It has an N-terminal and a C-terminal domain. The C-terminal domain consists of a biotin cofactor that is substrate-like. The role of the N-terminus of the biotin carrier is presently not completely elucidated. However, the N-terminal domain can attach and bind to biotin. The utilization and function of the N-terminus seems to link and fortify the carboxyl to biotin bond.

The ACCase enzyme is also crucial for increasing cell growth. The transfer of the carboxyl from the biotin protein carrier (BCCP) through the carboxyltransferase (CT) to acetyl-CoA is completed by two reactions [26]. The first half-reaction that uses the biotin carboxylase (BC) initiates the addition of a carboxyl to biotin through its covalent bond to the BCCP. The second reaction is catalyzed by CT, which repositions a carboxyl to acetyl-CoA and yields malonyl-CoA. By inhibiting the *accA* gene with a re-engineered IPTG-PT-asRNA vector, the absent CT subunit could not interact with BCCP. Less interaction

between BCCP and CT can lower the production of acyl-ACP from malonyl-ACP because less CT conversions of acetyl-CoA into malonyl-CoA would occur that are required to catalyze fatty acid synthesis and elongation of acyl-ACP. The complexes of acetyl-CoA carboxylase enzymes catalyze the carboxylase and transferase reactions. The carboxylase enzymes catalyze the addition of a carboxyl to a biotin prosthetic group of the biotin carboxylase carrier protein (BCCP) [9]. The carboxylase transferase (CT) also initiates and transports a carboxyl from the BCCP to an acyl group, which forms acyl thioesters.

Figure 8, Formation of Malonyl-CoA *(This figure was retrieved from reference 27 and originally published in the Journal of Biological Chemistry),* The acetyl-CoA carboxyl transferase, the AccA and AccD, and the alpha and beta subunits of the AccABCD complex transfers a carboxyl group from pyruvate to acetyl-CoA to form malonyl-CoA. Malonyl-CoA enters the fatty acid synthesis pathway, elongating fatty acids into long-chain fatty acids into phospholipids. The covalently bound biotin of BCCP carries the carboxylate moiety. A biotin carboxylase (BC) carboxylate an N1' atom of a biotin vitamin cofactor, utilizing ATP and carbon dioxide from bicarbonate. Biotin or vitamin H has a covalent bond to a lysine side chain residue located in the biotin carboxyl carrier protein or the BCCP subunit. The second step uses a carboxyltransferase (CT) to transfer carbon dioxide from a carboxybiotin to a carboxyl group. The CT moves the carboxyl group to acetyl-CoA, producing malonyl-CoA.

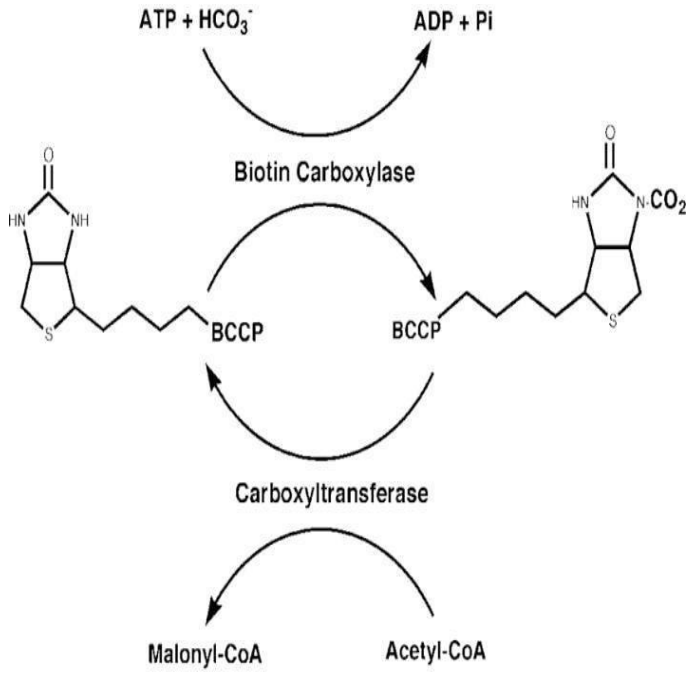

Inhibiting *accA*, lowered the expansion of fatty acid production because lessening ACCase activity shortens the length of the acyl chain, which can increase or decrease in elongation. Bacterial cells, in response to low temperatures or toxicity, can change the ratios of their acyl chains through saturation to unsaturation, from cis to trans-double-bonded carbons, and from branched to unbranched stacks of acyl chains [28]. Lipids are the central building blocks of the inner cytoplasmic membrane. Lipids maintain the structure of bacterial cells, increase survival, and increase growth by augmenting the passage of hydrophobic units via increased permeability. The lipid acyl chains that are produced during fatty acid elongation manufacture a more fluid and permeable bacteria cells (Fig 9).

Environmental fatty acids can also affect the fatty acids of the bacterial plasma membrane. *S. aureus* can absorb fatty acids from its environment and increase its rate of survival and growth even after antibiotic treatment of a fatty acid synthetic pathway. The biofilm of bacterial cells consists of larger concentrations of fatty acids that increase fluidity, isolating the bacterial community from a tumultuous environmental condition [28]. Fatty acid synthesis requires large quantities of energy and more access to phospholipids provided by the added glucose, which increases the activity of the ACCase enzyme. The asRNA inhibition of *accA* reduced the output of fatty acids that can negatively affect the biofilm yield and its composition.

Fatty acids stabilize the plasma membrane lipid bilayer for developing the early stages of biofilm. The metabolic fluxes that affect bacterial biofilm formation require further elucidation [13]. Biofilm causes a large portion of bacterial infections in hospitals known as nosocomial infections. Researchers treated mutant cultures with kanamycin and found that the biofilm showed a reduction in antibiotic resistance. However, after 250 generations, the resistant mutant bacteria increased by growth at the surface and the base of the biofilm [12]. Bacterial colonies within a biofilm are resistant to antibiotics. Because the extracellular biofilm matrix prevents the penetration of antibiotics, is mostly anaerobic, or lacking oxygen, bacteria within the biofilm are more tolerant of antibiotics [14].

Biofilm plays an intricate role in the genesis of infection and causes many nosocomial infectious diseases. Biofilm allows the movement of pathogenic bacteria to become more rapid and spread an infection into the blood circulation [40]. Bacterial cells in the biofilm have greater access to nutrients and oxygen than in a culture medium. Higher levels of fatty acids are present during the early growth phase. In addition, the large concentrations of DNA present in the biofilm serve to maintain a more cohesive matrix and a higher quality of the biofilm [41]. Bacterial cells located in the biofilm versus planktonic or free-living bacterial cells possess higher concentrations of fatty acids. The higher access of fatty acids increases tolerance to various temperatures, more stacking of bacterial cells, and a more stable lipid bilayer. A heightened presence of long-chain fatty acids leads to the increased orientation of fatty acids in

the lipid bilayer, amplifies the links between acyl chains, and stabilizes the lipid bilayer [28]. The fatty acids produced will form a more fluid membrane, and this fluidity causes the biofilm to expand. As the biofilm broadens, increased LuxS activity is needed to produce, and release AI-2 signals needed for the continuum of quorum sense activities. The number of bacterial microcolonies, through the AI-2/QS system, can transfer AI-2 signals that communicate cell-to-cell and amplify growth proportionally to the size of their extracellular matrix.

Figure 9 Long-Chain Fatty Acid Synthesis An acyl-group, or ACP, is added to the malonyl-CoA and converted into ketoacyl-ACP by an added carbon dioxide. The Beta- ketoacyl-ACP is reduced and gains hydrogen into Beta-hydroxyacyl-ACP. The Beta- hydroxyacyl-ACP is dehydrated, losing a molecule of water, to alter into Enoyl-ACP, which forms into Acyl-ACP by losing two hydrogen protons.

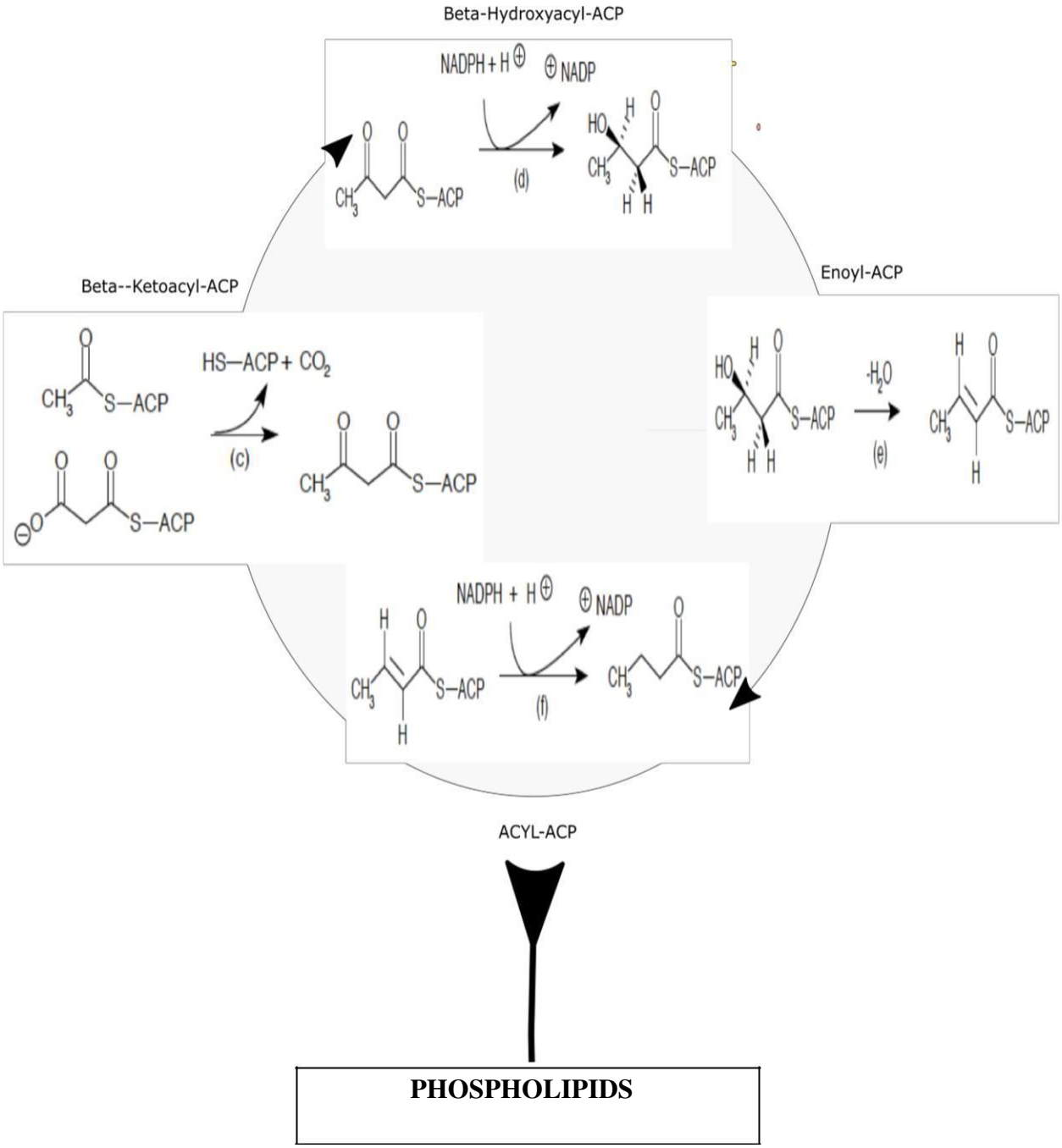

qPCR ANALYSIS OF *luxS* GENE EXPRESSION

LuxS synthesizes AI-2 QS signals needed to form biofilm, regulate gene expression, and release virulent factors. To determine the effect of *accA* inhibition on *luxS,* a qPCR analysis measured the number of l*uxS* gene copies after inhibiting *accA* while altering glucose availability. *Escherichia coli* cells were grown in 25µM and 5µM glucose and transformed with antisense pHN1257 expressing IPTG-PT-asRNA plasmids. Glucose increased the rate of transcription (Fig 10). Cell samples with 5µM glucose- (+)asRNA produced a high level of the *luxS* gene. The gene copy values of *luxS* for (+) glucose/ asRNA and (+) asRNA were quantified. For the results, (-) glucose-(+)asRNA samples produced a gene copy number of 199 and 2511 *luxS* copies for (-) glucose-(-)asRNA (n=3, 277 ± 37).

Adding 5µM glucose with *accA* knockout mutant cultures, increased *luxS* gene expression, which provided some uncertainty for the use of asRNA to fully eliminate the *accA* gene in vivo. However, asRNA of *accA* did lower the levels of *luxS* without glucose enhanced supplementation. For the 25µM glucose-(+)-*accA* asRNA and 5µM glucose (+)-asRNA-*accA* produced 39,810 and 316,228 gene copies of *luxS*, respectively. The control samples, (-) glucose-(-) asRNA (n=3, 658,114 ± 483,499) and 5µM glucose- (+) asRNA (n=3, 171571±204574) exhibited the highest level of *luxS* expression ($p<0.05$, $p=0.025$). Wang et al. (2005) found that adding 0.8% glucose to the bacterial culture and growth medium increased the activity at the promoter site of the *luxS* gene [29]. Jesudhasan et al. (2010) proved that higher levels of autoinducer-2 did not necessarily lead to increased gene expression of *luxS* for *Salmonella typhimurium* when cultured in excess concentrations of glucose [30].

The metabolism of carbohydrates also controls biofilm generation in many bacterial species [37]. For example, it was found that increased glucose availability allowed *S. epidermidis* to upregulate transcription specific for biofilm production during the stationary growth phase [38]. However, other bacteria from the *Enterobacteriaceae* species suppress the creation of biofilm as glucose availability increases. Many other gram-positive bacteria also repress biofilm formation in the presence of glucose. In bacterial species, *E. faecalis* augments its genesis of biofilm when glucose is in excess, but many different strains of *E. faecalis* can also repress biofilm construction while glucose is present [37]. The biofilm contains the total biomass of a bacterial community. The availability of nutrients determines the amount of biomass that accumulates within a biofilm. Adding glucose supplementation to the culture medium increases bacterial growth and total biomass [37].

Figure 10 Effect of glucose on the rate of transcription inhibition with asRNA and frequency of nucleic acid production A) from the control to 25 µM glucose exposure, bacteria cells transcribed DNA at an amplified rate. As the glucose concentration increased to 50 micromolar, the rate of transcription reached a sustained equilibrium with no new nucleic acid production or activity. B) asRNA caused gene inhibition of *accA.* The samples expressing asRNA inhibition of *accA* produced 16% (95% CI, [199, 1x10^6]) of the total yield of nucleic acids. Samples not represented asRNA inhibition yielded 83% (95% CI, [199, 1x10^6]) of the total amount of nucleic acids.

A.

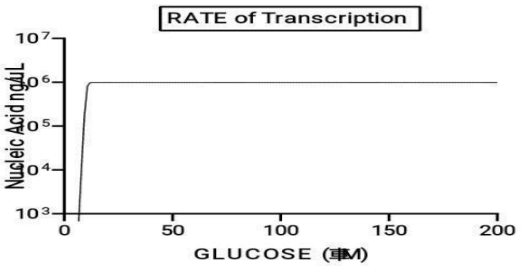

B.

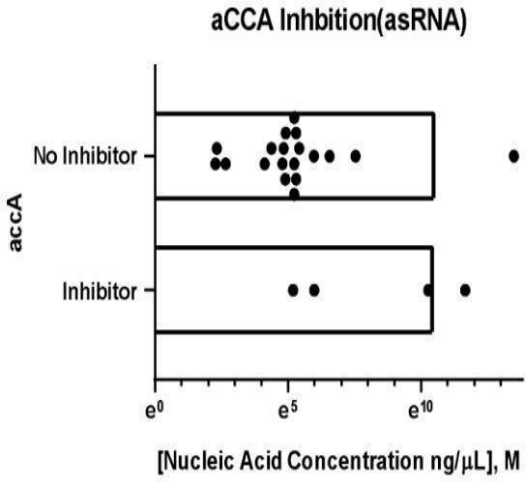

LuxS expression is an essential component for cell growth, quorum sense, and biofilm formation. The excess AI-2 sequesters and induces many bacterial cells to exchange AI-2 signals [35]. AI-2 fills the extracellular space when the bacterial population increases in growth [36]. Bacterial cells detect the excess AI-2, assess the cell density, and then signal the cessation of gene expression. Quorum-sense activity monitors and regulates gene expression through a positive feedback loop. This positive feedback is triggered by the peripheral and internal accumulation of AI-2. Quorum sense signals exchanged between bacterial cells monitors the genes responsible for organizing activities executed through different bacterial groups. Activities completed through quorum sense signaling include bioluminescence, spore formation, antibiotic excretion, creating biofilm, and releasing factors for virulence [36]. For example, the malfunctioning of *fsr* that resides in the quorum-sense gene locus for *E. faecalis* decreases biofilm formation [37].

Escherichia coli produces quorum-sense signals that regulate gene activity and growth. *Escherichia coli* and many gram-negative bacteria regulate the influx and output of AI-2. In *Escherichia coli*, the transporter and transmembrane complex called LsrABCD governs the uptake of AI-2. The repressor of LsrABCD and LsR is a kinase that is a part of the QS system of AI-2. Cyclic AMP/cyclicAMP receptor proteins regulate the *lsr* operon. The expression of cyclic AMP/cyclic AMP receptor proteins occurs by the positioning of *lsrK* and *lsrR* upstream of the *lsr* [31]. Lsrk that is a kinase located in the cytoplasm, phosphorylates AI-2, and then the Lsrk attaches to the *lsr* repressor.

In an intercellular process called quorum sense (QS) signaling, bacterial cells release AI-2 signaling molecules for detecting cell density and to regulate gene expression. Studies have shown AI-2 as a signaling molecule that regulates cellular processes in *Salmonella*. The activated AI-2 suppresses the *lsr* repressor, termed LsrR. After the activity of the *lsr* repressor is inhibited, the release of AI-2 increases via the autoinducer-activated expression of the Lux-S protein. AI-2 accumulates, monitors cell growth by permitting bacterial cells to sense the excess AI-2, and then terminate cell growth. Excess AI-2 distributes quorum sense signals between bacterial cells, which notifies cells of limited nutrients, surface area, or available space. AI-2 is dependent on the genetic expression and translation of *luxS* (Fig 11).

Figure 11 Regulatory mechanisms of the LsrR/phospho-AI-2 system in *E. coli* (Retrieved from reference 31). The AI-2 uptake repressor LsrR represses the *lsr* operon containing *lsrACDBFG* and the operon of *lsrRK*. AI-2 can re-enter the cell through the expression of LsrACDB. When the LsrK kinase phosphorylates an imported AI-2, the phosphorylated AI-2 binds to LsrR and terminates its repression of *lsr* transporter genes, inducing their expression. These regulatory steps trigger increased AI-2 uptake. (DPD=4,5-dihydroxy-2,3-pentanedione)**

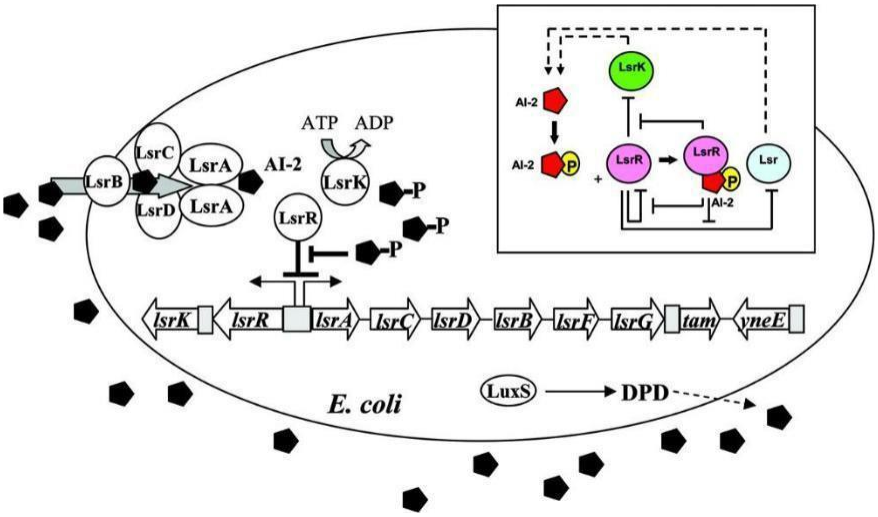

The inhibition of *accA* and decreasing the accessibility of glucose lowered the activity at the *luxS* promoter site. Lux-S is an AI-2-synthesizer. The escalating output of AI-2 amplifies *luxS* transcription. Widmer et al. (2012) found that the *luxS* mutant strain, PJ002, exhibited increased bacterial cell growth after adding 25µM of AI-2, which was not present in the phosphate-*buffered* saline or PBS buffer control solution [32]. The heightened genetic activity of *luxS* after glucose supplementation with or without the inhibition of *accA* can confirm the metabolic dependency of the LuxS/AI-2 QS system. Inhibiting *accA* and decreasing glucose lowered the expression of *luxS*. Less activity of the QS LuxS/AI- 2 system can reduce biofilm consistency and structure.

The reduced function of CT via *accA* extirpation can lessen the output of fatty acids that limit a bacterium's expression of virulence, initial adhesion to a surface, and its mobility [33]. When ablating *accA*, less *luxS* was produced where reduced fatty acid synthesis can decrease Lux-S expression (Fig 12). The declining activity of Lux-S can lower the release of AI-2. Less AI-2 reduces quorum sense activity that detects the cell density needed to escalate or block cell growth. Many bacteria form fatty acyl-homoserine lactones, or acyl-HSLs that operate as quorum-sensing signal molecules, which bind to signal receptors and monitor gene expression. The fatty acyl groups

are developed from fatty acid biosynthesis and elongation [34]. By inhibiting *accA* with asRNA interference, the acyl group formation was suppressed because *acc*A inhibition disrupted fatty acid elongation. Fewer acyl groups negatively affect the plasma membrane structures and biofilm of bacterial cells.

Hall et al. concluded that the cause of antibiotic resistance or antibiotic sensitivity of a biofilm originates from a genetic source [54]. The activity of *luxS* is linked to fatty acid synthesis and carbohydrate metabolism. Many pathogens express LuxS [49], and LuxS regulates bacterial metabolism while conducting many events of quorum sensing. Jia et al. found the growth and metabolism of the *luxS* mutant strain decreased because the reduction of fatty acid metabolic synthesis degraded cell membrane fluidity [55]. Inhibiting *accA* produced an incomplete fatty acid elongation cycle that suppressed the expression of *luxS* because the availability of fatty acids and acyl-groups decreased.

The author hypothesizes that disrupting FASII via *accA* inhibition can form an incomplete plasma membrane that reduces the cell membrane fluidity needed for the LsrACDB transmembrane protein to operate. A malfunctioning LsrACDB transmembrane protein can delay the influx of AI-2 for its phosphorylation required to initiate the LuxS/AI-2 QS system. The suppression of LsrACDB may have further reduced the internal concentration of AI-2. Less internal AI-2 may have downregulated *luxS* gene expression. The quality of the biofilm, a major cause of virulence, is largely determined by *luxS* expression. Therefore, the antibiotic susceptibility of gram-negative *E. coli* can rise because inhibiting *accA* to disrupt FASII breaks down the lipid bilayer of its IM (inner membrane). An incomplete PM of the inner membrane can permit an elevated influx of hydrophilic antibiotics into the cytoplasm of previously drug-resistant *E. coli*.

Hence, a higher awareness of the interaction between bacterial metabolic potency and virulence is needed [44]. According to Stokes et al., we are currently at the beginning stages of understanding the link between bacterial metabolism and antibiotic efficacy [45]. To connect bacterial metabolism with antibiotic susceptibility, the author attempted to integrate bacterial fatty acid synthesis with luxS activity. Increased glucose amplifies the production of acetyl-CoA carboxyltransferase. Increased glucose causes AI-2 quorum-sensing signal molecules to accumulate. The *accA* gene, translated into the AccA subunit of the acetyl-CoA carboxyl transferase enzyme (CT), transfers a carboxyl group from pyruvate to acetyl-CoA, forming malonyl-CoA. By increasing the glucose concentration in increments, Wang et al. found that glucose increased the levels of AI-2 in culture [29]. The proliferation of AI-2 augments the production of Lux-S.

Figure 12 *accA* affects *luxS* expression *accA* exhibits a proportional relation with *luxS*. A) As *accA* expression decreased during asRNA inhibition, *luxS* expression reduced in tandem. B) **The heat map shows** decreased *accA* (Dark Purple) values yielded higher Cp values for *luxS* (Neon Yellow). The highest Cp value of 20 was produced at position 13 for a Log_{accA} value approximately near 0. Less *luxS* DNA present is indicative of a higher CP value for *luxS* at a decreased *accA* expression level. C) Displays a logarithmic relation between *luxS* and log_{accA} that as *accA* approaches 0, the expression of *luxS* decreases. When *accA* reaches a threshold, *luxS* peaks, but then *luxS* reaches equilibrium as *accA* increases. D) The Cp Values for *luxS* were parallel and matched in a majority of log_{accA} data replicates. E) The QQ plot shows the means are normally distributed for *luxS,* Cp values, and log_{accA}. F) The sigmoidal plot shows a cooperative relation between accA and luxS.

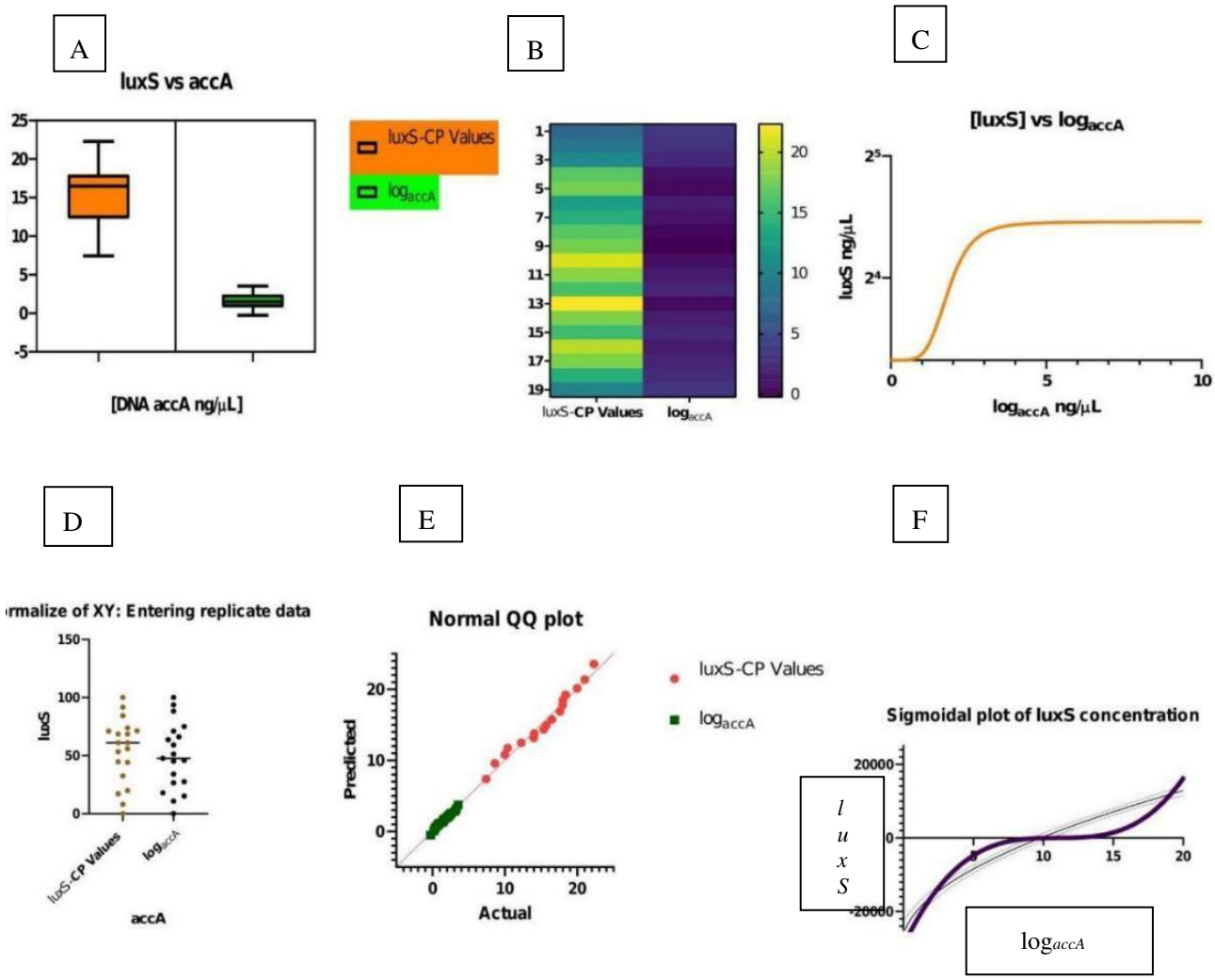

ANTIBIOTIC RESISTANCE TEST

An antibiotic resistance test was performed to determine the susceptibility of antibiotics from *E. coli* sample cultures expressing antisense RNA inhibition of the gene *accA.* The bacterial samples showing pHN1257-asRNA-*accA* gene suppression were predominantly susceptible to the antibiotic's tetracycline (10µg/mL), carbenicillin (100µg/mL), and chloramphenicol (25µg/mL) (Fig 13). Disks (N=64) consisting of each of the three antibiotics were placed on agar plates divided into eight sections. The zone of inhibition was measured in millimeters. For the experimental group (with asRNA), the median was 20 mm for the measurement of the zone of inhibition. The control groups (without (+)asRNA-accA) were mainly resistant to antibiotics, with an average of 6 mm ZOI. Bacteria transformed with pHN1257-(+)asRNA-*accA* were more susceptible to the antibiotic's tetracycline, carbenicillin, and chloramphenicol (Fig 14).

Fifty-nine percent of the experimental (+)asRNA-*accA* samples were sensitive to tetracycline, chloramphenicol, and carbenicillin (21±4, SEM=0.7). The (+)asRNA- *accA* treatment group displayed an intermediate sensitivity of 28% as 3% (95% CI, [6, 20]) were resistant to antibiotics (13.75±10, SEM=1.8). The control exhibited more resistance with 25%, 12.5%, and 53% of susceptibility, intermediate, and resistance, respectively. The (+) asRNA-*accA* treatment group had an 82% (95% CI, [6, 20]) difference in sensitivity compared to the (-)asRNA-*accA* control group. The control group showed 77% (95% CI, [6, 20]) variation in resistance when compared to the (+)asRNA-*accA* experimental group (p=0.000554). A paired t-test was performed, yielding a t-score of 3.6, and degrees of freedom equaling 31. The t-score and DF were used to calculate the p-value.

The antisense inhibition of *accA* disrupted fatty acid synthesis and elongation. Less access to viable fatty acids such as the acyl-ACPs led to an unstable plasma membrane structure for the *E. coli* cells. The incomplete plasma membrane then allowed the facile transport of the antibiotics, chloramphenicol, tetracycline, and carbenicillin to cross the double membrane of the gram-negative *E. coli* bacterial cells, which lowered its antibiotic resistance. The bacterium of *S. aureus* translates a lysine at its 164th genomic locus, forming an *S. aureus* that is resistant to the antibiotic called thailandamide. The thaillandamide also denatures and deactivates the AccA transferase subunit. The bacterium of *Salmonellae* also produces a mutation in the gene for *accA*. Other antibiotics, such as capistruin and malleilactone, are novel synthetic antibiotics that inhibit the transformation process between bacterial cells. This blockage of bacterial transformation causes increased production of antibiotics [42]. However, wild-type *S. aureus* incorporates exogenous and dissimilar fatty acids into its PM at significant phospholipid positions without the need for FASII antibiotic selection and this may cancel the previously assumed explanation for fatty acid selectivity of phospholipid-synthesizing enzymes [43].

In contrast, FASII antibiotic adaptation involves robust bacterial proliferation and incorporation of host fatty acids. Bacterial metabolism and environmental stress play concrete roles in the outcome of antimicrobial treatments [43]. Such metabolic fortitude allows bacteria to salvage metabolites from their environment. This consideration may limit the potential of selecting ACCs as metabolic targets for antimicrobial drug development. Exogenous fatty acids are converted into acyl-ACP in some gram-negative bacteria. The resulting acyl-ACP undergoes the same fate as endogenously synthesized acyl-ACP. Exogenous fatty acids are converted into acyl-phosphate in gram-positive bacteria and can be used for phospholipid synthesis or converted into acyl-ACP. Only *Lactobacillales* can use exogenous fatty acids to bypass FASII inhibition [39]. FASII shuts down entirely in the presence of exogenous fatty acids in *Lactobacillales*, allowing *Lactobacillales* to synthesize phospholipids entirely from exogenous fatty acids. Inhibition of FASII cannot be bypassed in other bacteria because FASII is only partially downregulated in the presence of exogenous fatty acids or FASII is required to synthesize essential metabolites such as β-hydroxyacyl-ACP [39].

The difference between mammalian and bacterial ACCase enzymes is vital for designing single-target antibiotics and antimicrobial gene knockout mutations of *accA*. An antibiotic designed to inhibit a bacterial ACCase enzyme cannot interfere or interact with a mammalian ACCase enzyme because the mammalian ACC isoforms differ from the bacterial ACCs. Mammals have a different isoform of ACC called ACC2 or ACCβ. ACCβ is conserved and matches 73% of its amino acids with the identity of isoforms ACC1 and ACC2 from humans [18]. ACC2 in mammals' functions as an enzyme located in the outer membrane of the mitochondria. ACC2 maintains a 140-residue orientation at the N-terminus. This 140-residue of amino acids located near the N-terminus is not present in the bacterial ACC [18]. The preceding 20 side chain residues of the 140 residues were almost wholly hydrophobic.

ACCase enzymes found in eukaryotes differ from those used by prokaryotes. In eukaryotic cells, BC has three domains, the A, B, and C domains. The side chain residue groups of A and C contain the active site. The domain of B enormously changes its conformation to cover the active site during the reaction. Eukaryotic cells have a BC domain with many partitioned and segmented residues. The side chain residues measure 550 residues between the BC and AB connecting domains as compared to bacterial BC units that contain 450 residues [18]. The subunits of the ACCase enzyme complex are favorable targets for antibiotic design because the bacterial ACCs are immensely different from mammalian and human ACC isoforms. Inhibiting bacterial ACCs cannot negatively modify or interfere with mammalian and human ACCase enzymes.

FIGURE 13 Zone of inhibition and Antibiotic Susceptibility Test
Bacteria that were transformed with pHN1257-(+)asRNA-*accA* showed greater susceptibility to the antibiotic disk containing tetracycline, chloramphenicol, and carbenicillin. Twenty-seven of the total 64 samples were susceptible to antibiotics. Eighteen of the samples were resistant, and 13 were only intermediate. The ratio of (+)asRNA-*accA* to (-)asRNA-*accA* equaled 3:2. B) Within the range of 20 to 22 mm of ZOI for the (+) asRNA-*accA* expressing bacteria, the antibiotic susceptibility showed a density of 0.01515. The control displayed less susceptibility at 20 to 30 mm ZOI with a density of 0.007.

A)

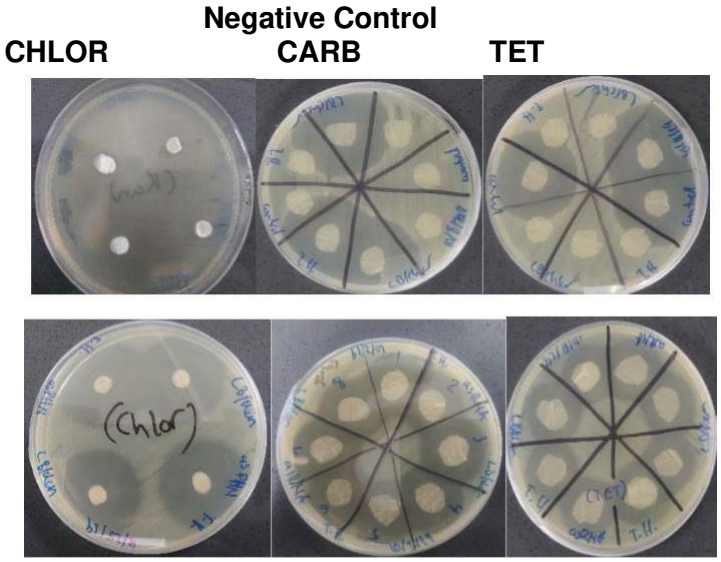

B)

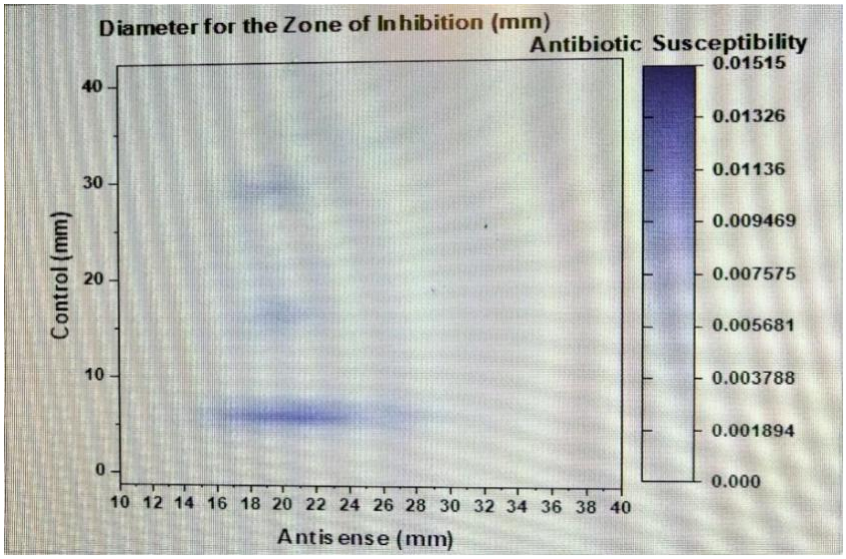

Figure 14 Zone of Inhibition A) There was a 60% (95% CI, [6, 20]) percent difference in the span of ZOI between the *accA*-mutant knockout and the control. The *accA* gene mutant showed a higher level of ZOI. B) The QQ plot exhibited a normal distribution of data residuals for the *accA*-mutant and the control. C) The heat map displays the control with a dominant green color and the *accA*- mutant produced darker hues as a black color. The green color for the control is an indicator of a lower level of ZOI and the darker hue as red and black of the *accA*-mutant specifies an elevated distance of ZOI. D) The homoscedasticity of residual data points is not maintained and is non-linear. E) The observed ZOI residual data points were different from the predicted ZOI for the *accA*-mutant and the control, demonstrating a non-linear regression.

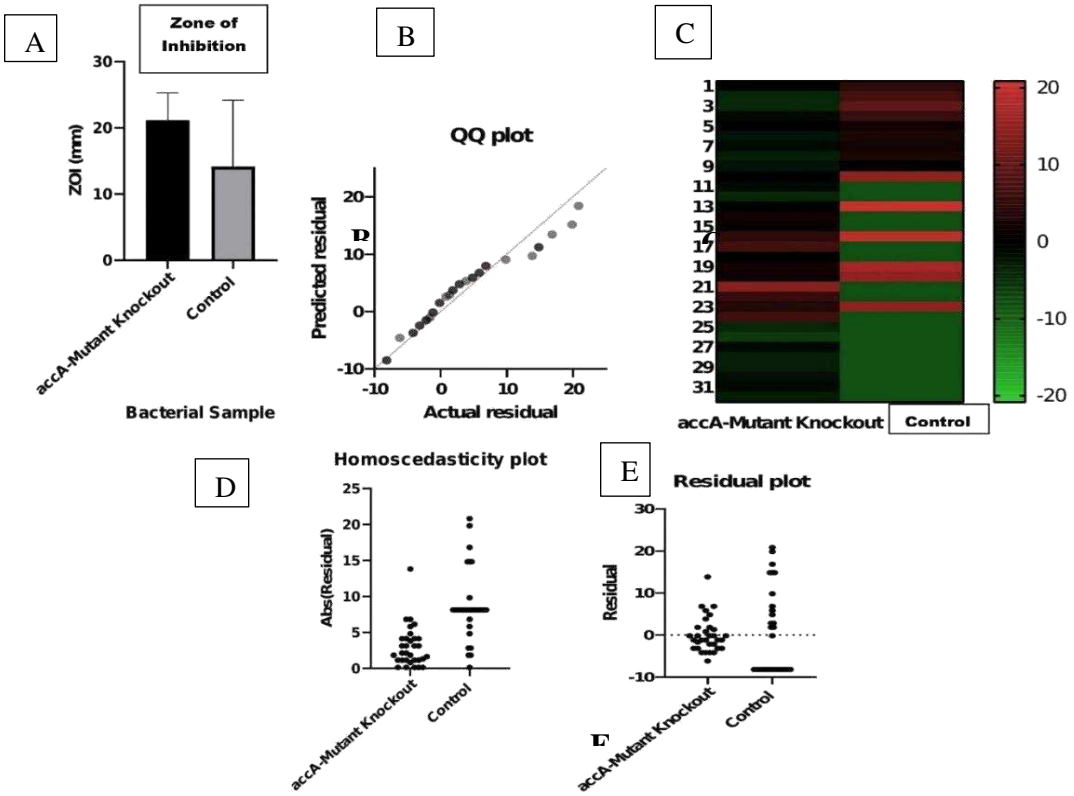

CONCLUSION

Multidrug-resistant Gram-negative bacteria (MDR-GNB) have created an intense challenge for clinicians treating infections of ill patients in intensive care units [56]. Higher rates of MDR-GNB is partially attributed to the double membrane of Gram-negative bacteria. The Gram-negative bacteria cell wall differs more than Gram-positive bacteria. Gram-negative bacteria have a cell envelope that contains an outer membrane consisting of LPS with endotoxins, a peptidoglycan cell wall, and an inner membrane. Gram-positive bacteria do not incorporate an outer membrane. The outer membrane can restrict the penetration of antibiotics into Gram-negative bacteria cells [60]. Only in current years has GNB become resistant to all common categories of antimicrobials [56].

Resistance of novel antibiotics have begun to rise, and administering these novel antibiotics has been limited to decrease any further occurrences of MDR. Recently, most drug companies have developed novel antimicrobials that have focused on Gram-positive bacteria. Many new and novel antibiotics have not been produced to combat Gram-negative bacteria [57]. The issue of MDR-resistant gram-negative bacteria and less new antibiotics to act against these MDR-GNBs have forced the administration of old antibiotics such as polymyxin B and polymyxin E. The polymyxins combat gram-negative bacteria such as Pseudomonas aeruginosa and *Enterobacter* species [58]. Antimicrobial peptides (AMPs) can degrade the bacterial structure by directly interacting with the membranes of microbes through electrostatic activity [59]. However, many AMPs have not achieved success in clinical studies because they are extremely toxic for mammalian cells.

Antimicrobial gene therapies may provide more novel antimicrobials for increasing antibiotic susceptibility of MDR gram-negative bacteria. The accA gene may represent a potential target for novel antimicrobial gene therapies. Because the DNA of the ACCase enzyme is conserved across many different species, targeting it with novel antibiotic-gene inhibition can eradicate the function and presence of the ACCase protein. Conserved DNA sequences do not mutate or change. If the DNA of the conserved sequence for the ACCase enzyme is inhibited or altered, then the enzyme will lack expression and completely lose its function.

This study presented important results for the effect of glucose and the inhibition of *accA* on *luxS*, an essential component of bacterial biofilm formation, quorum sense signaling, and virulence. *accA* encodes the AccA subunit of CT, which catalyzes FASII. Inhibiting accA decreased *luxS* gene expression. Suppression of luxS after silencing accA occurred because inhibiting *accA* lessened fatty acid production that decreased cell membrane fluidity. Disrupting quorum sense signaling was exhibited in the reduction of *luxS* after silencing accA. The expression of *luxS* is an essential factor of virulence. The qPCR absolute quantification results determined the total sum of gene copies for *luxS* decreased during *accA inhibition*. *E. coli* (+)asRNA-*accA* cell cultures produced 199 gene copies of *luxS* versus the control. The control yielded $1x10^6$ gene copies for luxS. Suppressing luxS can prevent biofilm formation and disrupt the LuxS/AI-2 QS system. Preventing biofilm creation and reducing QS activity can lessen the virulence of pathogenic bacteria. Bacteria that are highly virulent need to use biofilm for binding to epithelial cells and then spread infection.

The accumulation of AI-2 is used by bacteria to infect more host cells, and AI-2 creates a more solid biofilm [48]. The activity of the flagella is amplified with higher levels of *luxS* mutations present in the lungs and bloodstream. The mutant *luxS* allows bacteria to infect the lungs and blood more than the wild-type strain [49]. LuxS produces the DPD precursor for AI-2 synthesis [49]. The purpose of LuxS and AI-2 includes regulating metabolism and monitoring quorum sense activity [49]. The LuxS protein plays a significant role for generating infections [49]. The *luxS* gene, when it is more expressed, causes the spread of virulent bacteria by increasing the motility of pathogenic bacteria.

When Lux-S and AI-2 are less regulated and over-expressed, infectious bacteria can propagate in stressful environments with high acidity and salinity [51]. Kendall et al. (2008) demonstrated the ability of *S. pyogenes* to adapt to acidic conditions because of an upregulated Lux-S/AI-2 system [52]. The mutation of *luxS* in *Haemophilus influenzae* increases virulence and then causes middle ear infections [49]. The many facets of biofilm to tolerate antimicrobial therapy include many different types and subtypes of metabolic actions that regulate the bacterial response to different metabolic stimuli. The subtypes of metabolic changes include responses to pH, osmotic pressure, and the availability of nutrients [28].

The overall purpose of this study was to link bacterial metabolism such as the ACCase AccA-CT enzymatic catalysis of FASII with LuxS/AI-2 dependent virulence. The potent metabolic state of a bacterial population can inhibit bacterial susceptibility of antibiotics [47], therefore, suppressing bacterial metabolism may increase antibiotic sensitivity. E. coli cells expressing (+)asRNA-*accA* showed more susceptibility of antibiotics because asRNA blocked *accA* translation into AccA, which eliminated the AccA subunit from the ACCase-CT enzyme. A CT without AccA subunits cannot bind to carboxyls in order to catalyze FASII. Less FASII degrades the IM of gram-negative bacteria, and a damaged IM allows a more facile influx of hydrophilic antibiotics. However, there are limitations of this study where hydrophilic antibiotics could not be added to cell cultures during antibiotic susceptibility tests. If hydrophilic antibiotics were used, a more distinguished ZOI and percent difference between the experimental and control could have been shown. Hydrophilic antibiotics were not available at the time, but the antibiotic tests still exhibited higher rates of susceptibility for (+)-asRNA-*accA* cell cultures.

There is a significant link between bacterial cell metabolism and virulence. Understanding the metabolic dependency of bacterial virulence may become fundamental for designing novel antibiotics. There is a gap in the literature concerning the connection between bacterial metabolism and virulence. However, there is an immense possibility to design novel antibiotics that target bacterial-metabolic genes through antimicrobial gene therapies. Future research could design multiple novel antibiotics by identifying and targeting metabolic gene targets with antibiotic gene therapies. Hopefully, this study's

attempt to describe the interaction between fatty acid metabolism and virulence may add to our understanding of metabolic-dependent pathogenesis in bacteria.

ACKNOWLEDGMENTS Special thanks are given to the staff from TheLAB in Los Angeles, CA. Thank you for your team. They were always available for answering questions and providing support.

Funding: The author received no specific funding for this work.
Conflicts of interest: The authors declare no conflicts of interest.

REFERENCES

1. Polyak SW, Abell AD, Wilce MC, Zhang L, Booker GW. Structure, function, and selective inhibition of bacterial acetyl-CoA carboxylase. Applied microbiology and biotechnology. 2012 Feb 1;93(3):983-92.

2. Calero-Cáceres, W., Ye, M., & Balcázar, J. L. (2019). Bacteriophages as environmental reservoirs of antibiotic resistance. *Trends in microbiology*.

3. Lobanovska, M., and Pilla, G., 2017. Focus: Drug Development: Penicillin's Discovery and Antibiotic Resistance: Lessons for the Future?. *The Yale Journal of Biology and Medicine*, *90*(1), p.135.

4. Aminov, R., 2017. History of antimicrobial drug discovery: Major classes and health impact. *Biochemical pharmacology*, *133*, pp.4-19.

5. Landecker, H., 2016. Antibiotic resistance and the biology of history. *Body & Society*, *22*(4), pp.19-52.

6. Verstraeten, N., Knapen, W., Fauvart, M. and Michiels, J., 2016. A historical perspective on bacterial persistence. In *Bacterial Persistence* (pp. 3-13). Humana Press, New York, NY.

7. Eichenberger EM, Thaden JT. Epidemiology and Mechanisms of Resistance of Extensively Drug Resistant Gram-Negative Bacteria. Antibiotics. 2019 Jun;8(2):37.

8. Richie, D. L., Wang, L., Chan, H., De Pascale, G., Six, D. A., Wei, J. R., & Dean, C. R. (2018). A pathway-directed growth restoration assay to facilitate the discovery of lipid A and fatty acid biosynthesis inhibitors in Acinetobacter baumannii. *PloS one*, *13*(3).

9. Sweeney, P., Murphy, C. D., & Caffrey, P. (2016).

Exploiting the genome sequence of Streptomyces nodosus for enhanced antibiotic production. *Applied microbiology and biotechnology*, *100*(3), 1285-1295

10. N. Nakashima, T. Tamura. Conditional gene silencing of multiple genes with antisense RNAs and generation of a mutator strain of Escherichia coli. Nucleic Acids Res. 2009;103 (37).

11. Xu, L., Li, H., Vuong, C., Vadyvaloo, V., Wang, J., Yao, Y., Otto, M., and Gao, Q. Role Of the luxS quorum-sensing system in biofilm formation and virulence of Staphylococcus epidermidis. /14PeerJ reviewing PDF | (2018:12:33750: 1:2: NEW 8 Mar 2019) Manuscript to be reviewed Infection and immunity. 2006;74(1):488-496.

12. France, M. T., Cornea, A., Kehlet-Delgado, H., & Forney, L. J. (2019). Spatial structure facilitates the accumulation and persistence of antibiotic-resistant mutants in biofilms. *Evolutionary Applications*, *12*(3), 498-507.

13. Pisithkul, T., Schroeder, J. W., Trujillo, E. A., Yeesin, P., Stevenson, D. M., Chaiamarit, T., ... & Amador-Noguez, D. (2019). Metabolic remodeling during biofilm development of Bacillus subtilis. *MBio*, *10*(3), e00623-19.

14. Rojo-Molinero, E., Macià, M. D., & Oliver, A. (2019). Social behavior of antibiotic-resistant mutants within Pseudomonas aeruginosa biofilm communities. *Frontiers in Microbiology*, *10*, 570.

15. Peng B, Su YB, Li H, Han Y, Guo C, Tian YM, Peng XX. Exogenous alanine and/or glucose plus kanamycin kills antibiotic-resistant bacteria. Cell metabolism. 2015 Feb 3;21(2):249-62.

16. Broussard, T. C., Kobe, M. J., Pakhomova, S., Neau, D. B., Price, A. E., Champion,
T. S., & Waldrop, G. L. (2013). The three-dimensional structure of the biotin carboxylase-biotin carboxyl carrier protein complex of E. coli acetyl-CoA carboxylase. *Structure*, *21*(4), 650-657.

17. Broussard, T. C., Price, A. E., Laborde, S. M., & Waldrop, G. L. (2013). Complex formation and regulation of Escherichia coli acetyl-CoA carboxylase. *Biochemistry*, *52*(19), 3346-3357.

18. Tong, L. (2013). Structure and function of biotin-dependent carboxylases. *Cellular and Molecular Life Sciences*, *70*(5), 863-891.

19. Waldrop, G. L.; Rayment, I.; Holden, H. M. (1994). "Three-dimensional structure of the biotin carboxylase subunit of acetyl-CoA carboxylase". Biochemistry. **33** (34): 10249– 10256. *doi*:*10.1021/bi00200a004*. *PMID* 7915138.

20. Milke, L., Kallscheuer, N., Kappelmann, J., & Marienhagen, J. (2019). Tailoring Corynebacterium glutamicum towards increased malonyl-CoA availability for efficient synthesis of the plant pentaketide noreugenin. *Microbial cell factories*, *18*(1), 71.

21. Lietzan, A. D., & Maurice, M. S. (2013). A substrate-induced biotin binding pocket in the carboxyltransferase domain of pyruvate carboxylase. *Journal of Biological Chemistry*, *288*(27), 19915-19925.

22. Chandrakar, B., Jain, A., Roy, S., Gutlapalli, V. R., Saraf, S., Suppahia, A., ... & Nayarisseri, A. (2013). Molecular modeling of Acetyl-CoA carboxylase (ACC) from Jatropha curcas and virtual screening for identification of inhibitors. *journal of pharmacy research*, *6*(9), 913-918.

23. Bilder P, Lightle S, Bainbridge G, Ohren J, Finzel B, Sun F, Holley S, Al-Kassim L, Spessard C, Melnick M, Newcomer M, Waldrop GL. The structure of the carboxyltransferase component of acetyl-coA carboxylase reveals a zinc-binding motif unique to the bacterial enzyme. *Biochemistry* **45** 1712-22 (2006) doi:10.1021/bi0520479

23. Seti, Gita. (n.d). Discover Ideas about Protein. Retrieved from https://www.pinterest.com/pin/531002612291400564/ on June 30, 2020

24. Ikeda, M., Nagashima, T., Nakamura, E., Kato, R., Ohshita, M., Hayashi, M., & Takeno. (2017). In vivo roles of fatty acid biosynthesis enzymes in biosynthesis of biotin
and α-lipoic acid in Corynebacterium glutamicum.
Appl. Environ. Microbiol., *83*(19), e01322-17.

25. Salie, M. J., Zhang, N., Lancikova, V., Xu, D., & Thelen, J. J. (2016). A family of negative regulators targets the committed step of de novo fatty acid biosynthesis. *The Plant Cell*, *28*(9), 2312-2325.

26. Evans, A. L. (2018). The Distinctive Regulatory Mechanisms of Bacterial Acetyl- CoA Carboxylase.

27. Janiyani, K., Bordelon, T., Waldrop, G. L., & Cronan, J. E. (2001). Function of Escherichia coli biotin carboxylase requires catalytic activity of both subunits of the homodimer. Journal of Biological Chemistry, 276(32), 29864-29870.

28. Dubois-Brissonnet, F., Trotier, E., & Briandet, R. (2016). The biofilm lifestyle involves an increase in bacterial membrane saturated fatty acids. *Frontiers in microbiology*, *7*, 1673.

29. Wang, L., Hashimoto, Y., Tsao, C.Y., Valdes, J.J. and Bentley, W.E. Cyclic AMP (cAMP) and cAMP receptor protein influence both synthesis and uptake of extracellular autoinducer 2 in Escherichia coli. Journal of bacteriology. 2005;187(6):2066-2076.

30. Jesudhasan, P.R., Cepeda, M.L., Widmer, K., Dowd, S.E., Soni, K.A., Hume, M.E., Zhu, and Pillai, S.D. Transcriptome analysis of genes controlled by *luxS*/autoinducer-2 in Salmonella Enterica serovar Typhimurium.
Foodborne pathogens and disease.2010;7(4):399-410.

31. Li, J., Attila, C., Wang, L., Wood, T. K., Valdes, J. J., & Bentley, W. E. (2007). Quorum sensing in Escherichia coli is signaled by AI-2/LsrR: effects on small RNA and biofilm architecture. *Journal of bacteriology*, *189*(16), 6011-6020.

32. Widmer, K. W., Jesudhasan, P., & Pillai, S. D. (2012). Fatty acid modulation of autoinducer (AI-2) influenced the growth and macrophage invasion by Salmonella Typhimurium. *Foodborne pathogens and disease*, *9*(3), 211-217.

33. Nicol, M., Alexandre, S., Luizet, J. B., Skogman, M., Jouenne, T., Salcedo, S. P., & Dé,

E. (2018). Unsaturated Fatty Acids Affect Quorum Sensing Communication System and Inhibit Motility and Biofilm Formation of Acinetobacter baumannii. *International journal of molecular sciences*, *19*(1), 214. https://doi.org/10.3390/ijms19010214

34. Schaefer, A., Greenberg, E., Oliver, C. *et al.* A new class of homoserine lactone quorum- sensing signals. *Nature* **454,** 595–599 (2008).
https://doi.org/10.1038/nature07088
35.C.M. Waters, B.L. Bassler. Quorum sensing: cell-to-cell communication in bacteria. Annu. Rev. Cell Dev. Biol. 2005;21: 319-346.

36.S.T. Freestone, B.L. Bassler. Bacterial Quorum Sensing: Its Role in Virulence and Possibilities for Its Control. Cold Spring Harbor Perspectives in Medicine. 2012;2(11): a012427. doi:10.1101/cshperspect. a012427.

37. Pillai, S. K., Sakoulas, G., Eliopoulos, G. M., Moellering Jr, R. C., Murray, B. E., & Inouye, R. T. (2004). Effects of glucose on fsr-mediated biofilm formation in Enterococcus faecalis. *Journal of Infectious Diseases*, *190*(5), 967-970.

38. Dobinsky, S., Kiel, K., Rohde, H., Bartscht, K., Knobloch, J. K. M., Horstkotte, M. A., & Mack, D. (2003). Glucose-related dissociation between icaADBC transcription and biofilm expression by Staphylococcus epidermidis: evidence for an additional factor required for polysaccharide intercellular adhesin synthesis. *Journal of bacteriology*, *185*(9), 2879-2886.

39. Yao, J., & Rock, C. O. (2017). Exogenous fatty acid metabolism in bacteria. Biochimie, 141, 30-39.

40. Soares, A., Caron, F., & Etienne, M. (2019). Commentary: tolerance and resistance of pseudomonas aeruginosa biofilms to antimicrobial agents–how p. Aeruginosa can escape antibiotics. *Frontiers in Microbiology*, *10*, 2164.

41. Trappetti, C., Potter, A.J., Paton, A.W., Oggioni, M.R. and Paton, J.C. LuxS mediates iron-dependent biofilm formation, competence, and fratricide in Streptococcus pneumoniae. Infection and Immunity. 2011;79(11):4550-4558.

42. Wozniak CE, Lin Z, Schmidt EW, Hughes KT, Liou TG. Thailandamide, a fatty acid synthesis antibiotic that is coexpressed with a resistant target gene. Antimicrobial agents and chemotherapy. 2018 Sep 1;62(9):e00463-18.

43. Kénanian, G., Morvan, C., Weckel, A., Pathania, A., Anba-Mondoloni, J., Halpern, D., & Poyart, C. (2019). Permissive Fatty Acid Incorporation Promotes Staphylococcal Adaptation to FASII Antibiotics in Host Environments. Cell Reports, 29(12), 3974-3982.

44. Passalacqua, K. D., Charbonneau, M. E., & O'riordan, M. X. (2016). Bacterial metabolism shapes the host-pathogen interface. *Virulence Mechanisms of Bacterial Pathogens*, 15-41.

45. Stokes, J. M., Lopatkin, A. J., Lobritz, M. A., & Collins, J. J. (2019). Bacterial metabolism and antibiotic efficacy. *Cell metabolism*.

46. Baquero F, Martínez JL. Interventions on metabolism: making antibiotic- susceptible bacteria. mBio. 2017 Dec 29;8(6):e01950-17.

47. Jayaraman, A., Thomas, K.W. Bacterial quorum sensing: signals, circuits, and implications for biofilms and disease. Annu. Rev. Biomed. Eng. 2008; 10:145-167. 48.Vidal, J.E., Howery, K.E., Ludwick, H.P., Nava, P., and Klugman, K.P., 2013. Quorum-sensing systems LuxS/autoinducer two and Com regulate Streptococcus pneumoniae biofilms in a bioreactor with living cultures of human respiratory cells. Infection and immunity. 2013;81(4): 1341-1353.

49. Vendeville, A., Winzer, K., Heurlier, K., Tang, C.M., and Hardie, K.R., Making' sense of metabolism: autoinducer-2, LuxS, and pathogenic bacteria. Nature Reviews Microbiology. 2005;3(5):383.

50. Siller, M., Janapatla, R.P., Pirzada, Z.A., Hassler, C., Zinkl, D., and Charpentier, E., 2008. Functional analysis of the group A streptococcal *luxS*/AI-2 system in metabolism, adaptation to stress, and interaction with host cells. BMC microbiology. 2008;8(1), p.188.

51.M.M. Kendall, D.A. Rasko, V. Sperandio. Global effects of the cell-to-cell signaling molecule autoinducer-2, autoinducer-3, and epinephrine in a *luxS* mutant of enterohemorrhagic Escherichia coli." Infection and Immunity. 2007;75(10):4875-4884.

52. Vidal, J.E., Ludwick, H.P., Kunkel, R.M., Zahner, ¨ D. and Klugman, K.P. The LuxS dependent quorum-sensing system regulates early biofilm formation by Streptococcus pneumoniae strainD39. Infection and immunity. 2011;79(10):4050-4060.

53. Zuberi A*,* Misba L*,* Khan AU*.* CRISPR interference (CRISPRi) inhibition of luxS gene expression in E. coli: an approach to inhibit biofilm*. Frontiers in cellular and infection microbiology.* 2017 May *26;***7***:*214*.*

54. Hall CW*,* Mah TF*.* Molecular mechanisms of biofilm-based antibiotic resistance and tolerance in pathogenic bacteria*. FEMS microbiology reviews.* 2017 Mar *25;***41***(*3*):*276–301*.*

55. Jia, F. F., Pang, X. H., Zhu, D. Q., Zhu, Z. T., Sun, S. R., & Meng, X. C. (2017). Role of the luxS gene in bacteriocin biosynthesis by Lactobacillus plantarum KLDS1. 0391: A proteomic analysis. *Scientific reports*, *7*(1), 1-14.

56. *Bassetti M, Peghin M, Vena A, Giacobbe DR. Treatment of infections due to MDR Gram-negative bacteria. Frontiers in medicine. 2019 Apr 16;6:74.*

57. *Giamarellou H. Multidrug-resistant Gram-negative bacteria: how to treat and for how long. International Journal of Antimicrobial Agents. 2010 Dec 1;36:S50-4.*

58. *Falagas ME, Kasiakou SK, Saravolatz LD. Colistin: the revival of polymyxins for the management of multidrug-resistant gram-negative bacterial infections. Clinical infectious diseases. 2005 May 1;40(9):1333-41.*

59. *Lam SJ, O'Brien-Simpson NM, Pantarat N, Sulistio A, Wong EH, Chen YY, Lenzo JC, Holden JA, Blencowe A, Reynolds EC, Qiao GG. Combating multidrug-resistant Gram-negative bacteria with structurally nanoengineered antimicrobial peptide polymers. Nature microbiology. 2016 Sep 12;1(11):1-1.*
60. *Exner M, Bhattacharya S, Christiansen B, Gebel J, Goroncy-Bermes P, Hartemann P, Heeg P, Ilschner C, Kramer A, Larson E, Merkens W. Antibiotic resistance: What is so special about multidrug-resistant Gram-negative bacteria?. GMS hygiene and infection control. 2017;12.*